ESTIMATION OF FRACTURE TOUGHNESS AND CRACK GROWTH BEHAVIOUR OF C-M_n STEEL WELDMENT

A DISSERTATION

Submitted in partial fulfilment of the requirements for the award of the degree of

MASTER OF ENGINEERING

in

MECHANICAL ENGINEERING

(With Specialization in Welding Engineering)

By

DUMENDRA KUMAR THAKUR

DEPARTMENT OF MECHANICAL AND INDUSTRIAL ENGINEERING
UNIVERSITY OF ROORKEE
ROORKEE–247 667 (INDIA)

FEBRUARY, 2001

CANDIDATE'S DECLARATION

I hereby declare that the work which is being presented in the dissertation entitled, **"ESTIMATION OF FRACTURE TOUGHNESS AND CRACK GROWTH BEHAVIOUR OF C-Mn STEEL WELDMENT"** in the partial fulfil ment of the requirements for the award of the degree of **MASTER OF ENGINEERING** in **MECHANICAL AND INDUSTRIAL ENGINEERING** with specialization in **WELDING ENGINEERING,** submitted in the **DEPARTMENT OF MECHANICAL AND INDUSTRIAL ENGINEERING, UNIVERSITY OF ROORKEE, ROORKEE,** is an authentic record of my own work carried out from July 2000 to February 2001 under the supervision of **SHRI. AJAI AGARWAL**, Lecturer, Department of Mechanical and Industrial Engineering, University of Roorkee, Roorkee (India).

The matter embodied in this dissertation has not been submitted by me for the award of any other degree or diploma.

D Thakur.

Dated: Feb. 28, 2001

(DUMENDRA KUMAR THAKUR)

This is to certify that the above statement made by the candidate is correct to the best of my knowledge.

Ajai Agg

(Shri Ajai Agarwal)

Lecturer,

Dept. of Mech. and Ind. Engg.

University of Roorkee

Roorkee - 247 667 (India)

ACKNOWLEDGEMENT

It is distinct pleasure to acknowledge my deep and sincere gratitude to ***Shri Ajai Agarwal,*** *Lecturer, Department of Mechanical and Industrial Engineering, University of Roorkee, Roorkee for his valuable suggestions, necessary guidance and keen interest at all stages of this work.*

I am grateful to all staff members of the department for the knowledge imparted during the course of my study at this university.

I would take the opportunity to thank the technical staff of WELDING RESEARCH LABORATORY, MIED for providing me all the help during my experimental work.

Last but not least, I would like to express my sense of indebtedness to Mr. Manish Saraswat, my friends and all those who directly or indirectly helped me in the whole Dissertation work.

D Thakur

Roorkee ***(DUMENDRA KUMAR THAKUR)***

Feb.25, 2001 *M.E. –FINAL YEAR*

WELDING ENGG.

ABSTRACT

For this study work weld metal were deposited with the combination of Grade C-Mo wire and Automelt Grade iv Flux on C-Mn Steel using Submerged Arc Welding process. Mechanical properties, Charpy V-notch energy, Hardness, Fatigue crack growth rate and fracture toughness (J_{IC}) tests were performed on weld metal as well as base metal.

More Strength and less ductility was found in case of weld metal as compare to base metal. Toughness was assessed using the Charpy V-notch Impact test. Toughness of weld metal was found considerably high even at –30 °C temperature.

The resistance of fatigue crack propagation of weld metal and base metal were evaluated at room temperature in Air. Fatigue crack growth rates were determined, as a function of the stress intensity factor range and value of Paris constants were determined for the stress ratio of 0.1 and 0.3. The crack propagation rate was higher in weld metal as compare to base metal which might be attributed to residual stress present in weld. Threshold stress intensity factor range was also found more in weld metal as compare to base metal.

The weld metal had superior Fracture Toughness (J_{IC}) compare to base metal. This might be due to repeated re-heating, refining and tempering of the weld metal microstructure during the fabrication of weld.

CONTENTS

LIST OF TABLES

LIST OF FIGURES

NOMENCLATURE

SAW	:	Submerged Arc Welding.
LEFM	:	Linear Elastic Fracture Mechanics.
EPFM	:	Elastic-Plastic Fracture Mechanics.
HAZ	:	Heat Affected Zone.
BM	:	Base Metal.
WM	:	Weld Metal.
FCGR	:	Fatigue Crack Growth Rate.
Mpa	:	Mega Pascal.
Mo	:	molybdenum.
Mn	:	Manganese.
C	:	Carbon.
da/dN	:	Fatigue Crack Growth Rate.
R	:	Stress Ratio.
a	:	Crack Length.
a_o	:	Initial Crack Length.
a_f	:	Final Crack Length.
a_c	:	Critical Crack Length.
Δa_p	:	Stable Crack Extension.
σ_{ys}	:	Yield Stress.
σ_{us}	:	Ultimate Stress.
σ_f	:	Flow Stress.
N	:	No. of Cycles

K_{max}	:	Max. Stress Intensity Factor.
ΔK	:	Stress Intensity Factor Range.
ΔK_{th}	:	Threshold Stress Intensity Factor Range.
c,m	:	Material Constants for Paris Equation.
C_1, C_2	:	Constant for J_R-Curve.
K_{IC}	:	Plane Strain Fracture Toughness.
J_{IC}	:	Fracture Toughness (Crack initiation energy).
E	:	Modulus of Elasticity.
ν	:	Poisson Ratio.
B	:	Specimen Thichness.

CHAPTER - 1

INTRODUCTION

Weld design has become more quantitative by the development of fracture mechanics, which basically deals with characterizing the interaction between material stress level and tolerable crack size to produce a fracture resistance design of any large complex structure [7].

The life of structural components that contain cracks or that develop cracks early in their life may be governed by the rate of sub-critical crack propagation. In general, it is recognized that welded joints always contain some discontinuities and cracks. Moreover, proof testing or non-destructive testing procedures or both may provide information regarding the relative size and distribution of possible pre-existing cracks prior to service. However, these inspection procedures are used to establish upper limits on undetectable defect size. Thus to establish the minimum fatigue life of welded structural components, it is reasonable to assume that the component contains the largest discontinuity that cannot be detected by the inspection method [18].

The useful life of these structural components is determined by the fatigue crack-growth behaviour of the material. Therefor to predict the minimum fatigue life of structural components and to establish safe inspection intervals, an understanding of the rate of fatigue crack propagation is required. The most successful approach to the study of fatigue crack propagation is based on the fracture mechanics concepts [19].

As all welded structures contain flaws or cracks, engineering design requires determination of maximum flaw size for safe operations. Large flaw could lead to unstable crack

propagation and ultimately to structure failure. Knowledge of fracture toughness of the material, a measure of its resistance to unstable crack propagation, is required for engineering design [7].

C-Mn Steel is the most widely used material in components in structures, hence the knowledge of fracture toughness and fatigue crack growth behaviour of weld deposit of this metal under dynamic loading is of great importance in recent days of technologies for the quality assessment of weld joint.

CHAPTER - 2

LITERATURE REVIEW

Engineering structure of all kind, including welded structure have been braking unexpectedly in service for as far back as record are available and until comparatively recently effective methods for assessment and control of fracture were simply not lavailable. Development of new discipline called fracture mechanics has proceeded by rather subtle stages and as a consequence the underlying basis of the various techniques[7].

2.1 CRACK GROWTH BEHAVIOUR

During process of fatigue failure, micro cracks initially form and then coalesces to grow to micro cracks, which propagate until the fracture toughness of the material is exceeded and final fracture occurs. So the fatigue life of a structural components is determined by the sum of the elapsed cycles required to initiate a fatigue crack and to propagate the crack from sub-critical dimensions to the critical size consequently the fatigue life of structural components may be considered to be composed of three continuous stages [19]:

1. Fatigue - crack initiation
2. Fatigue - crack propagation , and
3. Fracture

2.1.1 Fatigue Crack Initiation

Under normal loading conditions, fatigue cracks are known to initiate at or near singularities on or just below the surfaces of metals. Such singularities may be inclusions, embrittled grain boundaries, sharp scratches or slip bands. The tragedy of the fatigue resistance of metals is that even when the surfaces of metals are highly polished and no stress concentrators are present, if the alternating stress amplitude is sufficiently high, slip band forms. This lead to slip

steps on the surface, intrusions, extrusions, hills, valleys or grooves, which in turn lead to initiation of small micro cracks. Even fatigue cracks that initiate near inclusions often seem to be on slip band that impinge on the inclusions new- -man has given a model for fatigue-crack initiation along coarse slip lives that does not require extrusions as shown in Fig 2.3. During tension, alternate slip on two interesting slip system is required for the mechanism to operate. As the tensile stress is increased, slip on first system is activated and then assumed to stop because of work hardening, the second system has becomes active. During decrease of the tensile stress, the excess dislocations on the active slip lanes are assumed to run out, creating the crack [19].

2.1.2 Fatigue - Crack Propagation

Fatigue cracks initiate in local slip bands and initially tend to grow in a plane of maximum shear range. This growth is quite small, usually of the order of several grains covering a max distance of a few mm. As the cycling of load continues the fatigue cracks tend to join and grow along planes of maximum tensile stress range.

Crack propagation data may be obtained from a number of specimens. Starting with a mechanically sharpened crack, cyclic load is applied and the resulting change in crack length monitored and recorded as a function of the no of cycles.

It is important note that the crack growth most often increases with the increasing crack length. It is most significant that the crack becomes longer and increasingly more rapid rate, thereby shortening component life at an alarming rate. An important corollary of this fact is that most of the loading cycles involved in the total life of an engineering component are consumed during the early stages of crack extension when the crack is small and perhaps undetected [19].

2.1.3 Fracture

As the crack progresses the stress on the residual cross section increases so that there is a corresponding increase in the rate of crack propagation. Ultimately, a stage is reached when the remaining area is unable to support the applied load and final rupture occurs.

2.2 FATIGUE ANALYSIS WITH LEFM APPROACH

The linear elastic fracture mechanics (LEFM) approach is based on the assumption that a defect is already present in the material and the analysis is to predict when this defect will reach the critical size and the catastrophic failure of the component will occur. The main contribution of LEFM is the stress intensity factor K, expressed as[9]

$$K = \phi \sigma \sqrt{\pi a} \qquad (1)$$

Where ϕ is a geometry factor dependent on the a/w ratio and a is half crack length. W is the width of the specimen and σ is applied stress. In case of pulsation load the stress intensity factor range, ΔK, is obtained from above equation with σ replaced by $\Delta\sigma$. Considering a body with an initial crack length a_i, subjected to pulsation load, the crack grows with increasing number of load cycles. At any given crack length a, the rate of crack propagation, da/dN can be computed. The relation between da/dN (mm/cycle), and the corresponding stress intensity factor range ΔK, $(MPa\sqrt{m})$, gives a straight line relation on the log - log plot over a wide range. In this region a power function of the type.

$$\frac{da}{dN} = c\,(\Delta k)^m \qquad (2)$$

is valid. c and m are constants. This relation, known as *PARIS EQUATION*, is found to be valid for all metallic materials in the crack growth range of approximately 10^{-6} to 10^{-3} mm cycle. However, at lower, and higher valves of da/dN the relation tends to become parallel to the Y axis,

thus resulting in a sigmodal type of curve as shown in Fig 5. The stage I which shows the initial growth of a long crack is very much structure sensitive. It depends on the Ratio (σmin/ σmax). The stage II where Paris relation is valid, is not very much dependent on the structure or yield strength of the material. The third stage is governed by the fracture toughness K_{IC} of the material

The main advantage of LEFM approach is that the fatigue life N_f can be easily obtained through the Paris equation thus.

$$\int_{a_i}^{a_f} d_a/(a)^{m/2} = c(\phi)^m(\Delta k)^m \int_{o}^{N_f} dN \qquad (3)$$

The crack length integrated from its value a_i to the final fracture length a_f and the corresponding number of cycles from zero to N_f.

2.3 FRACTURE TOUGHNESS

Fracture toughness is a property of the metal, which defines its resistance to brittle fracture. All engineering materials can be divided into four types from point of view of fracture toughness [16]. These are-

1. Linear elastic materials of low yield strength, i.e. brittle material for example glass.
2. Linear elastic materials of high strength e.g. HSLA Steels, high strength Aluminium and Titanium alloys.
3. Elastic-Plastic materials like mild steels
4. Highly Plastic materials like lead.

Fracture toughness of brittle material is determined by the use of *Griffith-Irwin* criterion for plane strain condition, while crack resistance curve provides the corresponding energy based criterion for plane stress condition.

In case of elastic plastic material of high strength a small plastic zone is formed at the end of crack, resulting in resistance to crack propagation thus resulting in higher toughness of material. Fracture toughness in such material for plane strain condition is determined by linear elastic fracture mechanics (LEFM). Which is now a very developed and well established procedure [16].

The plastic zones created at crack tip of propagating crack in elastic plastic materials are much larger than can be accounted for by LEFM treatment. Fracture toughness for such materials is determined by techniques such as crack opening displacement (COD), J-integral and R-curve.

Generally materials of very high toughness do not have high strength so are much less used in conditions warranting brittle fracture. No specific method exists for determining fracture toughness of such high toughness material [16].

2.4 ELASTIC-PLASTIC FRACTURE MECHANICS

Elastic-Plastic analysis techniques serve to purposes. First, they allow the prediction of cracking initiation and growth potential in components and structures and second they allow the determination of an elastic fracture parameter from small specimens which can be converted to a linear elastic parameter and then used directly in elastic fracture analysis.

J-integral:

The J-integral provides a relatively simple means to determine the energy release rate for a case where a large plastic zone exists at the crack tip. Thus this technique can be used to estimate the fracture characteristics of materials exhibiting elastic plastic behaviour and is a means of extending LEFM concepts from Linear elastic (K_{IC}) behaviour to elastic plastic behaviour [21].

J-integral can be defined as a mathematical expression, a line or surface integral that encloses the crack from one crack surface to the other, used to characterize fracture toughness of a material having appreciable plasticity before fracture. The J-integral eliminates the need to describe the behaviour of the material near the crack tip by considering the local stress-strain field around the crack front. J_{IC} is the critical value of the J-integral required to initiate growth of a pre-existing crack [2].

$$J = \int_{\Gamma} \left(wdy - T.\frac{\partial y}{\partial x} ds \right) \qquad (5)$$

Where T is the traction vector defined by the normal, along the integration path T. ds is an increment of length along the integration path. ω is the strain energy density defined for non linear elastic material.

2.5 FAILURE ASSESSMENT

The main theoretical justification for using J as a failure parameter comes from the work of Mcclintock [15]. A simple analytical form for J in the presence of large scale yielding can be obtained using a strip yielding model, which gives-

$$J = J_1 \frac{8}{\Pi^2} \left(\frac{\sigma_1}{\sigma} \right)^2 \ln \sec \left(\frac{\Pi \sigma}{2\sigma_1} \right) \qquad (6)$$

Where J_1 is the value of J determined linear elastically and σ_1 is plastic collapse stress.

Typical curve of $(J/J_1)^{1/2}$ against (σ / σ_1) is shown in fig. 2.6. This curve can be used to predict the failure load of a cracked structure when J_{IC} is known. Choose a value of σ, determine $(J/J_1)^{1/2}$ and enter the ordinate at this value. Then read off the value of σ/σ_1, which corresponds to

this on the relevant curve. The failure load is when this σ value equals to the originally chosen value. Similarly if the failure load is known, J_{IC} can be determined [5].

2.6 FAILURE ASSESSMENT DIAGRAM

Definition:

The failure assessment diagram is another way expressing the failure line derived from strip yielding model. It basically deals with two criterion approch:

1. Total Brittle Fracture : $K_I = K_{IC}$

2. Total Ductile Fracture : $\sigma = \sigma_L$ or $(K_I < K_{IC})$

Fig. 2.5 represents the conditions for these failures. Equation 6 forms the basis of a failure assessment diagram. This is based on the two parameters K_r and S_r, where

$K_r = K_I / K_c$ and

$S_r = \sigma / \sigma_I$

These forms the ordinate and abscissa of a failure diagram. It is clear from the eq. that curve

$$K_r = \left[\frac{8}{\pi^2 S_r^2} \ln \sec\left(\frac{\pi}{2} S_r\right)\right]^{-\frac{1}{2}} \qquad (7)$$

is a failure line on this diagram corresponding to the locus of failure points. If K_r and S_r are evaluated for a loaded cracked structure they provide an assessment point on the diagram with coordinates (K_r, S_r). If this point falls on or outside the curve then failure is predicted. If it falls inside the curve structure is safe [5].

Validation:

The concept behind the failure curve and the use of a modified strip yielding model solution can be validated by plotting experimentally measured fracture data on the failure diagram as shown in fig. 2.8. It can be seen from the fig. 2.8 that the experimental data scatter about the

failure assessment curve. To establish a lower bound failure criterion the failure line is reduced in size by 15%(dashed curve). All the experimental points fall outside this line demonstrating that the failure assessment diagram provides safe failure prediction when used in conjunction lower bound material properties [5].

2.7 RELEVANT TESTING STANDARDS

2.7.1 Fatigue Crack Growth Rate Test (ASTM E-647) [1]

Scope

This test method covers the determination of study state fatigue crack growth rate from near threshold to K_{max} controlled instability using compact type C-T specimen. Results are expressed in terms of the crack tip stress intensity factor range.

Significance and Use

(1). Fatigue crack growth expressed as a function of stress intensity factor range, da/dN versus ΔK, characterizes a material resistance to stable crack extension under cycle loading. Expressing da/dN as a function of ΔK provides results that are independent of planes geometry. Thus, enabling exchange and comparison of data obtained from a variety of specimen configuration and loading conditions.

(2) This test method can serve the following purposes :

(a) To establish the influence of fatigue crack growth on the life of components subjected to cyclic loading provided data are generated under representative conditions and combined with appropriate fracture toughness data.

(b) To establish material selection criteria and inspection requirements for damage tolerant applications.

(3) Expressing da/dN as a function of ΔK provides results that are independent of planar geometry, thus enabling exchange and comparison of data obtain from a variety of specimen configurations and loading conditions. Moreover, this feature enables da/dN versus ΔK data to be utilized in the design and evaluation of engineering structures.

(4) Residual stress can have an influence on fatigue crack growth behaviour. The effect can be significant when test specimens are removed from material in which complete stress relief is impractical such as weldments, as quenched materials and complex forged or extruded shapes. Residual stress superimposed on the applied stress can cause the localized crack tip. Stress intensity factor to be different than that computed solely from externally applied loads [1].

Specimen order Size Requirement

In order for result to be valid according to this method, it is required that the specimen be predominantly elastic at all values of applied load. The minimum in-plane specimen sizes to meet this requirement are based primarily on empirical results and are specific to specimen configuration. For C(T) specimen the following is required [1]:

$$(w\text{-}a) \geq (4/\pi)\,(K_{max}/\sigma_{ys})^2$$

where (w-a) = specimen un-cracked ligament

σ_{ys} = yield strength

K_{max} = Stress intensity factor corresponding to maximum load

Test Method:

This test method involves cyclic loading of notched specimens, which have been acceptably pre-cracked in fatigue. Crack length is measured as a function of elapsed fatigue

cycles. These data are subjected to numerical analysis to establish the rate of crack growth. Crack growth rates are expressed as a function of the stress intensity factor range ΔK, which is calculated from the expression based on Linear Elastic stress analysis.

Determination Of Stress Intensity Factor Range, ΔK [1]:

For C(T) specimen ΔK is given as

$$\Delta K = \frac{\Delta P(2+\alpha)}{B\sqrt{W}(1-\alpha)^{3/2}}[0.886 + 4.64\alpha - 13.32\alpha^2 + 14.72\alpha^3 - 5.6\alpha^4]$$ Where α

=a/w. Expression valid for a/w ≥0.2.

2.7.2 J_{IC}(A Measure of Fracture Toughness) E-813-89 [1]

Scope

This test method covers the determination of J_{IC}, which can be used as an engineering estimate of fracture toughness near the initiation of slow stable crack growth for metallic materials. It applies specifically to geometries that contain notches and flaws and that are sharpened with fatigue cracks. The recommended specimens are generally bend type that certain deep initial cracks. The loading rate is slow and environmentally assisted cracking is assumed to be negligible [1].

Significance

1) The property of J_{IC} determined by this test method characterizes the toughness of materials near the onset of crack extension from a pre-existing fatigue crack
2) The J_{IC} value marks the beginning stage of material crack growth resistance development, the full extent of which is not evaluated y this test method.

Test Method:

The objective of J_{IC} procedure is to determine the value of J near the initiation of crack growth. The method involves three point bend loading of fatigue pre-cracked specimens and determination of J as a function of crack growth load versus load-line displacement is recorded digitally or auto-graphically on x-y recorder. The J-integral is determined and plotted against physical crack growth, Δap using atleast four data points within specified limits of crack growth. These data reflects the materials resistance to crack growth, The J versus crack growth behaviour is approximated with a best fit power law relationship. A blunting line is drawn, approximating crack tip stretch effect. The blunting line is calculated from material flow properties.An offset line parallel to blunting line but offset by 0.2mm is drawn and the intersection of this line and the power law fit gives provisional J_{IC} (J_Q), which defines Jic, provided validity requirement of this test method are satisfied. Two techniques are described in ASTM E-813 to obtain J as a function of crack growth. The first technique requires four or more identically prepared specimens tested to different crack opening displacement and plotted as a single curve to obtain the desired plot. This technique is called the "multiple specimen techniques" and utilizes optical measurement of physical crack length. The second technique requires only one specimen and is called "single specimen technique" and uses elastic compliances or an equivalent indirect method to evaluate the specimen crack length [1].

Data Evaluation:

Calculation of J-integral are made from load, load point displacement curve obtained using the procedure outlined in chapter 3 in section 3.7.5.At a given total deflection, the area under

the load displacement curve is calculated. Area are than converted to energy unites according to the load scale and displacement scale used. The result are expressed in joules.

Calculation of J is done according to

$$J = J_{el} + J_{pl}$$

Where

J_{el} = Elastic component of J and

J_{pl} = Plastic component of J.

For three point bending specimens

$$J = \frac{(K)^2(1-\nu^2)}{E} + J_{pl}$$

Where

$$K = \frac{PS}{\sqrt{BB_N}(W)^{3/2}} f(a/w)$$

With

$$F(a/w) = \frac{3\alpha^{1/2}}{2(1+2\alpha)(1-\alpha)^{3/2}}[1.99 - \alpha(1-\alpha)(2.15 - 3.93\alpha + 2.7\alpha^2)]$$

$$J_{pl} = \frac{2A_{pl}}{B_N b_o}$$

Where A_{pl} = Area under load displacement curve

B_N = Net specimen thickness

b_o = (w-a_o) and

S = Bend span = 4W

Validation of J_Q as J_{IC} :

$J_Q = J_{IC}$ if

1. Thickness $B > 25\, J_Q / \sigma_{ys}$.
2. Initial ligament $b_o > 25\, J_Q / \sigma_{ys}$.
3. The slope of the power law regression line, dJ/da, evaluated at Δa_Q is less than σ_{ys}.
4. No specimen demonstrated brittle cleavage fracture at the applicable test temperature and rate.

Use

1) J_{IC} can be used to evaluate materials in terms that can be significant to design. The value of J_{IC} may be used as a ductile fracture toughness criterion to evaluate the effect of metallurgical variables, heat treatments and weldments.

2) This test method can be used in a service evaluation to establish the suitability of a material for a specific application for which stress conditions are prescribed and for which inspection flow size limits can be established with confidence. In case where the onset of flaw stable crack growth, as opposed to maximum

CHAPTER-3

EXPERIMENTATION

3.1 BASE MATERIAL

In the present work C-Mn Steel was used as base metal. Size of each plate to be welded was 500 mm X 125 mm X 25 mm. Four such plates were welded along their length, so as to make a weldment of size 500 mm X 250 mm X 25 mm. Chemical composition of this material is shown in Table No. 3.1.

3.2 FILLER MATERIAL

Filler material used is a high Mn-Moly Steel wire. Diameter of electrode wire used was 3.15 mm.It is manufactured by Advani-Oerliken, India with specification as AS-4Mo which confirms to IS:7280-1974 and class ED-1 of AWS A5.23-1976.

Chemical composition of filler wire is shown in Table No 3.2.

3.3 FLUX

Specification of flux used for welding is

Trade Name : Automelt Grade-IV Flux

Made by : Advani-Oerlikon Ltd.

Type of flux : Agglomerate Ca-Silicate type high basicity flux

Chemical composition of weld metal is shown in Table No 3.3.

3.4 WELDING MACHINE

Specification of Submerged Arc Welding machine used is:

Name	:	Unite LE-18 (Messere-Grishem)
Voltage Range	:	0-60 V
Current Range	:	0-1500 A
Travel Speed Range	:	0-120 cm/min

3.5 WELDING OF PLATES

3.5.1 Groove Preparation

Each plate of size 500 mm X 125 mm X 25 mm was machined at the edge in order to obtain a double V-groove with root face of 3 mm. A complete groove design is shown in fig. 3.2.

3.5.2 Baking of Flux

The flux was baked at 300 ^{o}C for one hour before use.

3.5.3 Welding Parameters

Plates were welded using multi pass welding. Welding parameters are as follows:

Current	:	500 A
Voltage	:	28 V
Travel Speed	:	35 cm/min
No Of Passes	:	4
Polarity	:	DCSP.

3.6 PREPARATION OF TEST SPECIMENS

Various specimens having dimensions as shown in fig. 3.3 to fig. 3.6 were prepared. These specimens were:

1. Tensile test specimens (According to ASTM E-8M)
2. Impact test specimens(According to ASTM E-23)
3. C(T) specimens for FCGR test(According to ASTM E-647)
4. TPB specimens for J_{IC} test (According to ASTM E-813)
5. Specimen for hardness test.

3.7 MECHANICAL TESTINGS

Various mechanical tests, carried out in this work can be broadly classified into two major headings namely conventional mechanical tests and fracture mechanics tests. Conventional tests include smooth tensile, charpy V-notch and hardness (HV5) tests. Fracture mechanics tests include fatigue crack growth rate and fracture toughness tests. Fig.3.1 shows the schematic view of experimental plane.

3.7.1 Tensile Tests

Tensile test were carried out as per ASTM -8M using smooth bar tensile test specimens having dimensions as shown in fig. 3.3.

Before starting the tensile test, the diameter of each specimen was measured and gage length of 45 mm was marked on the specimens. Specimen was fixed firmly into the jaws of the machine. Load was applied and increased gradually till fracture occurred. Yield load and Ultimate load were obtained from the load displacement curve. Using tensile test data Yield strength,

ultimate strength, % elongation and % reduction in area were calculated. Total 6 specimens, 3 of base metal and 3 of all weld metal were tested using this procedure.

3.7.2 Impact Tests

Charpy V-notch impact tests were carried out as per ASTM E-23. Impact tests of base as well as weld metal were carried out at temperatures –30 ^{o}C, -15 ^{o}C, 0 ^{o}C and 10 ^{o}C (Room Temperature).Two specimens were tested at each temperature.

3.7.3 Hardness Tests

Hardness of the welded specimens was determined by Vickers method on WOLPERT hardness tester. A load of 5 kg was applied to the specimen and a prism shaped diamond indentor was allowed into the test piece. After completion of the test, diagonals of impression of indentor were measured and the corresponding (HV-5) hardness value was taken from the standard chart. Impressions were taken on base metal, HAZ and weld metal at various points along the transverse section of etched specimens.

3.7.4 Fatigue Crack Growth Rate Tests

The fatigue crack growth rate tests of base and weld metal were carried out using C(T) specimens in a pulsater in accordance with ASTM E-647.

The specimen surface was polished to allowed visual identification of the crack tip. Testing was done in air at room temperature (13 ^{o}C) at a cyclic stress frequency of 5Hz. In the test the fatigue crack was initiated and propagated under tension to tension sinusoidal loading for different stress ratio, R. Prior to making crack length measurement,

The fatigue crack was extended up to 3.5 mm from the notch root. Load corresponding to K_{max} equal to 22 MPa$\sqrt{m}$ for base metal and 25 MPa$\sqrt{m}$ for weld metal were used to cause initial pre cracking at the machined notched, later on the load was stepped down. The fatigue crack growth

was measured with the help of a travelling microscope. Number of cycles elapsed for every 0.5 mm crack length extension were recorded. Paris law constants (c & m) for base and weld metal were calculated.

3.7.5 Fracture Toughness Tests

Fracture toughness (J-integral) tests were conducted on 600 KN servo hydraulic machine controlled by MTS system. Specimens tested were of three point bending type. Multiple specimen technique was used for obtaining J-R curve. Six specimens from base metal and eight from weld metal were tested. Specimens were pre-cracked up to a a/w ratio of 0.6. Pre-cracking was done at 0.5 P_l. Where $P_l = \frac{4}{3}\frac{Bb_o^2\sigma_{ys}}{S}$. After pre-cracking specimens were loaded to different displacement levels for required crack extension. Loading rate was 0.02 mm per second in displacement mode. Load displacement curve was plotted on X-Y plotter. Specimens were loaded to different displacement levels of 40, 50, 60, 70, 80, 90, 100, 110, percent of maximum displacement, where maximum displacement was the displacement where first significant load drop occurred. After loading up to desired displacement level specimens were unloaded. For crack marking all the specimens were heat tinted at 300 ^{o}C for 20 minute and then broken by continuous increasing static loading.

Sectioning of broken specimens was done to make the specimen size suitable for microscopic study. Initial and final crack length measurement was made on microscope with magnification of 16X.

CHAPTER-4

RESULTS AND DISCUSSION

4.1 TENSILE TESTS

The mechanical properties such as Yield strength, Ultimate strength, %Elongation, %Reduction of area of the weld as well as base metal are tabulated in Table No. 4.2. These properties are also schematically shown by bar chart in fig. 4.3 and fig. 4.4. This chart indicates that Yield strength and Ultimate Strength of weld metal is more as compared to base metal, while % Elongation and % Reduction of area is less in case of weld metal as compare to base metal. This change in properties may be attributed to presence of higher percentage of Mn and Mo.

4.2 IMPACT TESTS

Energy absorption in the charpy V-notch impact test at the temperature –30 ^{o}C , 15 ^{o}C , 0 ^{o}C and 10 ^{o}C (Room Temperature), carried out on weld as well as base metal are shown in Table No. 4.4. These results are schematically represented in fig.4.6. The results show that even at –30 ^{o}C temperature weld metal absorbed a significant amount of energy of the order of 50 Joules, while at this temperature energy absorbed by the base metal was 12 Joules. Since Mo has a tendency to refine the grains results in an increase in toughness, hence increase in toughness of weld metal could be attributed to presence of Molybdenum.

4.3 HARDNESS TESTS

Hardness behaviour across the weld is shown in fig. 4.5 and results are tabulated in Table No. 4.3. Weld metal was found more hard as compared to base metal and HAZ. Molybdenum present in weld metal might cause this increase in hardness.

4.4 FATIGUE CRACK GROWTH RATE TESTS

Two specimens of base metal and two specimens of weld metal, one for each stress ratio (R=0.1 & R=0.3) were tested for FCGR study. All the tests were carried out at room temperature.

Data concerning to crack size, No of cycles, ΔK, da/dN for C-Mn Steel and its weld for both stress ratio, were presented in tabular form in Table No. 4.6 to 4.9. From these data graphs between ΔK and da/dN on log-log scale were plotted for each tests. These plots are shown in fig. 4.7 to fig. 4.9. From these graphs value of Paris Constants (m & c) were evaluated.

These graphs were plotted, using Microsoft Excel and from where the equation of best-fit line was obtained. The slope of the best-fit line gives the value of 'm' and intercept of this line with Y-axis gives the value of 'c'. These values of m & c were found out for each case and presented in tabular form in Table No 4.10.

Though it requires some more specimens to be test, to conclude anything but analysis of the plots of FCGR and values of m & c at different stress ratios indicates that the value of 'm' increases with increase in stress ratio R, while value of 'c' decreases with increase in stress ratio R, for both C-Mn Steel as well as its weld.

These tests data shows that with increase in stress ratio overall fatigue crack growth rate increases and these is in confirmation to the Literature Review. The value of Threshold stress intensity factor range for base metal is higher as compare to base metal. These test data also shows that FCGR in weld sample is higher than that in base metal sample. This higher FCGR in weld metal might be attributed to residual stresses present in weld metal.

4.4 FRACTURE TOUGHNESS (J_{IC}) TESTS

Base Metal:

Fig. 4.11 to 4.16 shows the load displacement curve of all six base metal specimens. Initial crack and final crack size readings for each specimen are given in Table No. 4.11. Fig. 25 shows a typical photograph showing the stable crack extension. From load displacement curves value of J was evaluated using formula given in section 2.7.3 of Chapter-2.Calculations for J evaluation were done and summary of these calculations for each specimens is as follows:

Scale for load displacement curve

X-axis	1 small division	= 1/28 mm
Y-axis	1 small division	= 0.29 KN
Area	1 mm^2 =0.29X1/28	= 10.357 N-mm
		=10.357 Joules.

Here for all base metal specimens:

σ_{ys}	=	255 Mpa
σ_{us}	=	400 Mpa
E	=	200 Gpa
ν	=	0.3
B	=	20 mm
W	=	40 mm
S	=	160 mm

Specimen B-1:

Energy (A_E)	=	27.77 Joules
Max. Load (P)	=	16.2 KN
Average initial crack length (a_o)	=	24.5855 mm
Average final crack length (a_f)	=	25.0622 mm
Crack extension (Δa_p)	=	0.4767 mm
f(a/w)	=	3.994
K	=	64.74 MPa$\sqrt{m}$
J_{pl}	=	180 KJ/m^2
J_{el}	=	19.07 KJ/m^2
J	=	199.07 KJ/m^2

Specimen B-2:

Energy (A_E)	=	32.37 Joules
Max. Load (P)	=	15.57 KN
Average initial crack length (a_o)	=	24.768 mm
Average final crack length (a_f)	=	25.423 mm
Crack extension (Δa_p)	=	0.655 mm
f(a/w)	=	4.067
K	=	63.32 MPa$\sqrt{m}$
J_{pl}	=	214.8 KJ/m^2
J_{el}	=	18.24 KJ/m^2
J	=	233.04 KJ/m^2

Specimen B-3:

Energy (A_E)	=	43.645 Joules
Max. Load (P)	=	15.66 KN
Average initial crack length (a_o)	=	25.14 mm
Average final crack length (a_f)	=	26.2 mm
Crack extension (Δa_p)	=	1.06 mm
f(a/w)	=	4.225
K	=	66.163 MPa$\sqrt{m}$
J_{pl}	=	293.7 KJ/m^2
J_{el}	=	19.92 KJ/m^2
J	=	313.62 KJ/m^2

Specimen B-4:

Energy (A_E)	=	54.665 Joules
Max. Load (P)	=	15.28 KN
Average initial crack length (a_o)	=	25.113 mm
Average final crack length (a_f)	=	26.371 mm
Crack extension (Δa_p)	=	1.568 mm
f(a/w)	=	4.213
K	=	64.374 MPa$\sqrt{m}$
J_{pl}	=	367.2 KJ/m^2
J_{el}	=	18.85 KJ/m^2
J	=	386.05 KJ/m^2

Specimen B-5:

Energy (A_E)	=	64.39 Joules
Max. Load (P)	=	14.665 KN
Average initial crack length (a_o)	=	25.132 mm
Average final crack length (a_f)	=	27.128 mm
Crack extension (Δa_p)	=	1.996 mm
f(a/w)	=	4.22
K	=	61.886 MPa$\sqrt{m}$
J_{pl}	=	433 KJ/m^2
J_{el}	=	17.42 KJ/m^2
J	=	450.42 KJ/m^2

Specimen B-6:

Energy (A_E)	=	71.7 Joules
Max. Load (P)	=	13.8 KN
Average initial crack length (a_o)	=	25.3833 mm
Average final crack length (a_f)	=	27.6922 mm
Crack extension (Δa_p)	=	2.309 mm
f(a/w)	=	4.333
K	=	59.8 MPa$\sqrt{m}$
J_{pl}	=	490.53 KJ/m^2
J_{el}	=	16.27 KJ/m^2
J	=	506.8 KJ/m^2

J_R–Curve:

J-integral values obtained from above calculations are plotted against the corresponding measured stable crack extension (Δa_p) values. A power law curve of type

$$J = C_1(\Delta a_p)^{C_2}$$

was fitted through these points which is known as J_R –Curve. The value of C_1 and C_2 obtained was-

C_1 = 302

C_2 = 0.589

Fracture Toughness:

A blunting line is drawn as per ASTM E-813 with equation $J = 2\sigma_y(\Delta a_p)$. The intersection of the 0.2 mm offset line and J_R-curve gives the value of J_{IC}. Here it was obtained for base metal as:

J_{IC} = 210 KJ/m^2

Weld Metal:

Fig. 4.17 to 4.24 shows the load displacement curve of all eight weld metal specimens. Initial crack and final crack size readings for each specimens are given in Table No. 4.14. Fig. 26 shows a typical photograph showing the stable crack extension. From load displacement curves value of J was evaluated using formula given in section 2.7.3 of Chapter-2.Calculations for J evaluation were done and summary of these calculations for each specimens is as follows:

Here for all base metal specimens:

σ_{ys} = 420 Mpa

σ_{us} = 508 Mpa

E	=	200 Gpa
ν	=	0.3
B	=	20 mm
W	=	40 mm
S	=	160 mm

Specimen W-1:

Energy (A_E)	=	36.27 Joules
Max. Load (P)	=	19.66 KN
Average initial crack length (a_o)	=	25.335 mm
Average final crack length (a_f)	=	25.895 mm
Crack extension (Δa_p)	=	0.56 mm
f(a/w)	=	4.312
K	=	84.76 MPa$\sqrt{m}$
J_{pl}	=	247.33 KJ/m^2
J_{el}	=	32.68 KJ/m^2
J	=	280.01 KJ/m^2

Specimen W-2:

Energy (A_E)	=	44.77 Joules
Max. Load (P)	=	22.14 KN
Average initial crack length (a_o)	=	24.0 mm
Average final crack length (a_f)	=	24.701 mm
Crack extension (Δa_p)	=	0.701mm
f(a/w)	=	3.771

K	=	83.49 MPa$\sqrt{m}$
J_{pl}	=	279.8 KJ/m^2
J_{el}	=	31.7 KJ/m^2
J	=	311.5 KJ/m^2

Specimen W-3:

Energy (A_E)	=	48.7 Joules
Max. Load (P)	=	19.32 KN
Average initial crack length (a_o)	=	24.081 mm
Average final crack length (a_f)	=	25.2 mm
Crack extension (Δa_p)	=	1.121 mm
f(a/w)	=	3.772
K	=	72.84 MPa$\sqrt{m}$
J_{pl}	=	305.9 KJ/m^2
J_{el}	=	14.1 KJ/m^2
J	=	330 KJ/m^2

Specimen W-4:

Energy (A_E)	=	58.9 Joules
Max. Load (P)	=	21.68 KN
Average initial crack length (a_o)	=	24.918 mm
Average final crack length (a_f)	=	26.134 mm
Crack extension (Δa_p)	=	1.216 mm
f(a/w)	=	4.13

K	=	89.54 MPa$\sqrt{m}$
J_{pl}	=	390.53 KJ/m^2
J_{el}	=	136.48 KJ/m^2
J	=	426.48 KJ/m^2

Specimen W-5:

Energy (A_E)	=	63.49 Joules
Max. Load (P)	=	20.0 KN
Average initial crack length (a_o)	=	24.304 mm
Average final crack length (a_f)	=	26.05 mm
Crack extension (Δa_p)	=	1.746 mm
f(a/w)	=	3.88
K	=	77.6 MPa$\sqrt{m}$
J_{pl}	=	404.5 KJ/m^2
J_{el}	=	27.42 KJ/m^2
J	=	431.92 KJ/m^2

Specimen W-6:

Energy (A_E)	=	80.62 Joules
Max. Load (P)	=	22.3 KN
Average initial crack length (a_o)	=	24.654 mm
Average final crack length (a_f)	=	26.581 mm
Crack extension (Δa_p)	=	1.927 mm
f(a/w)	=	4.02

K	=	89.64 MPa$\sqrt{m}$
J_{pl}	=	525.3 KJ/m^2
J_{el}	=	36.56 KJ/m^2
J	=	561.86 KJ/m^2

Specimen W-7:

Energy (A_E)	=	84.69 Joules
Max. Load (P)	=	21.3 KN
Average initial crack length (a_o)	=	24.912 mm
Average final crack length (a_f)	=	26.886 mm
Crack extension (Δa_p)	=	1.957 mm
f(a/w)	=	4.13
K	=	87.97 MPa$\sqrt{m}$
J_{pl}	=	561.3 KJ/m^2
J_{el}	=	32.21 KJ/m^2
J	=	596.51 KJ/m^2

Specimen W-8:

Energy (A_E)	=	96.146 Joules
Max. Load (P)	=	18.96 KN
Average initial crack length (a_o)	=	25.79 mm
Average final crack length (a_f)	=	29.22 mm
Crack extension (Δa_p)	=	3.43 mm
f(a/w)	=	4.524

$K = 85.77\ MPa\sqrt{m}$

$J_{pl} = 676.6\ KJ/m^2$

$J_{el} = 33.47\ KJ/m^2$

$J = 710.07\ KJ/m^2$

J_R–Curve:

The value of C_1 and C_2 obtained for weld metal was-

$C_1 = 389$

$C_2 = 0.54$

Fracture Toughness:

A blunting line is drawn as per ASTM E-813 with equation $J = 2\sigma_y(\Delta a_p)$. The intersection of the 0.2 mm offset line and J_R-curve gives the value of J_{IC}. Here it was obtained for weld metal as:

$J_{IC} = 270\ KJ/m^2$

Crack initiation energy (J_{IC}) for weld metal was found high as compared to base metal. This might be attributed to presence of Mo in weld metal, the repeated reheating, refining, and tempering of weld metal microstructure.

CHAPTER-5

CONCLUSION

1 Yield strength and Ultimate strength of weld metal has been found more than that of base metal, while percentage elongation and percentage reduction of area has been found less in weld metal than that of base metal.

2 Hardness in weld metal has been found maximum. Hardness decreases in the order WB>HAZ>BM.This may be attributed to presence of Mo in weld metal.

3 Energy absorbed during fracture in case of weld metal has been found considerably high, in the order of 50 Joules even at -30° C, while that for base metal at -30° C is 12 Joules. This may be attributed to presence of Mo in weld metal.

4 FCGR is higher in weld metal as compared to base metal. This may be due to residual stresses present in weld metal.

5 In FCGR tests value of m increases and value of c decreases and overall rate of fatigue crack growth increases with an increase in stress ratio.

6 Threshold stress intensity factor range has been found more for weld metal as compared to base metal.

7 For weld metal value of c is less and value of m is more as compared to that for base metal. Hence at lower value of stress intensity factor range is higher in base metal and for higher value of stress intensity factor range crack growth rate is higher in weld metal.

8 Weld metal has lower crack initiation energy, J_{IC} value than that of the base metal. This might be attributed to repeated reheating, refining and tempering of weld metal microstructure during fabrication of multi pass weld. Mo present in weld metal may also help in refining of grains.

CHAPTER-6

SCOPE FOR FUTURE WORK

1 The experimental determination of J-integral is exhaustive. It requires a lot of specimen to be tested and a lot of time consumption. This can be determine mathematically by finite element method using some software like ANSYS.

2 HAZ is a very critical region in any weldment hence a fracture mechanics study can be done on this zone also.

3 Multipass welding is uneconomical but it improves the mechanical properties, hence a study on effect of number of passes on fracture toughness and FCGR can be done and a compromise between economy and mechanical properties can be determined.

REFERENCES

1. Annual book of ASTM Standards, 1990, Section 3, Metal Test Method and Qualitical Procedure.
2. ASM hand book, "Failure Analysis and Prevention", Vol-11, 1996.
3. ASM hand book, " Fracture and Fatigue", Vol-19,1996
4. Banks E. "Toughness Properties of HAZ Structures in Structural Steel", Welding Journal, Vol-53, No. 7, 1974, PP-299-S.
5. Chell G.G., "Elastic-Plastic Fracture Mechanics", Development in Fracture Mechanics, vol. 1, 1979, pp-67.
6. Fatigue and micro structure, papers presented at the 1978 ASM materials science seminar.
7. Gray T.G.F. and Spence J, "Rational Welding Design", Second Edition Chapter 5 (pp-217) and Chapter 6 (pp-308).
8. Hasson D.F., Zanis C.A. Anderson D.R., "Fracture Toughness of HY-130 Steel Weld Metals", Welding Journal, Vol-63, No.6, 1984 (pp-197-S).
9. Knott J.F., "Fundamentals of Fracture Mechanics",1973, pp-150.
10. Koo J.Y. "Welding metallurgy of structural steels", proceeding of an International Symposium on welding metallurgy of structural steels, Feb. 22-26, 1987, (pp 255-302).
11. Larsson L.H, "Subcritical crack growth due to fatigue, stress corosion and creep".
12. Linnert E. George, "Welding Metallurgy", AWS, vol. 1,Third Edition,1965.
13. Maddox S.I. "Assessing the significance of flaws in weld subjected to fatigue", welding journal, Vol. 53, No. 9, 1974 (pp 401-S).
14. Mcclintock F.A., "Fracture", vol. 3, 1971.

15. Milne, "Failure Assessment", Development in Fracture Mechanics, vol. 1, 1979, pp-259.

16. Parmar R.S., "Welding Engineering and Technology", Second Edition, 1994.

17. Rading G.O. "The effect of Welding On the Fatigue Crack Growth Rate in a Structural Steel" welding journal, vol - 72, No.7, 1993, (pp 307-S).

18. Richard W. Hertzberg, "Deformand and fracture mechanics of Engineering materials".

19. Rolfe and Barsom, "Fracture and Fatigue Control in Structure".

20. Stout R.D. "Weldability of Steels" Chapter 4 PP (131-136).

21. Turner C.E., Latzko D.G.H.,Hellen T.K., "Post Yield Fracture Mechanics", Second Edition, 1979.

Table No. 3.1: Chemical composition of Base Metal

%C	%Mn	%S	%P	%Si
0.15	0.9	0.03	0.03	0.3

Table 3.2: Chemical composition of filler wire*

%C	%Mn	%S	%P	%Si	%Mo
0.07-0.12	1.6-2.0	0.03	0.03	0.3	0.45-0.65

Table 3.3: Chemical composition of weld metal*

%C	%Mn	%S	%P	%Si	%Mo
0.1	1.4-1.9	0.03	0.03	0.5	0.5

*As given by manufacturer.

Table No. 4.1: Tensile test data of C-Mn Steel and Its Weld

Dimensions/ Properties	Notation	Unit	Base Metal			Weld Metal		
			Sp. 1	Sp. 2	Sp.3	Sp. 1	Sp. 2	Sp.3
Initial Diameter	D_o	mm	9.02	9.01	9.2	9.04	8.96	9.02
Initial Gage Length	L_o	mm	45	45	45	45	45	45
Final Fracture Dia.	D_f	mm	5.56	5.64	5.74	5.9	5.9	6.1
Final Gage Length	L_f	mm	59.8	56.7	56.6	54.7	44.46	54.4
Initial C.S. Area	A_o	mm^2	81.36	82.81	84.64	81.72	80.28	81.36
Final C.S. Area	A_f	mm^2	30.91	31.80	32.94	34.81	34.81	37.21
Yield Load	P_{ys}	KN	21.0	20.8	21.5	35.1	33.7	33.6
Ultimate Load	P_{us}	KN	33.0	33.1	33.4	42	40.4	41.3
Yield Stress	σ_{ys}	N/mm^2	258.0	251.2	254.0	429.3	419.8	412.9
Ultimate Stress	σus	N/mm^2	405.6	399.7	394.6	513.9	503.2	507.6
% Elongation over 45mm Gage length	E	%	32.8	26.0	25.77	21.5	21.0	21.0
% Reduction of Area	ROA	%	62.0	61.6	61.1	57.4	55.64	54.0

Table No. 4.2: Tensile properties of C-Mn Steel and its Weld

Material	Yield Stress (MPa)	Ultimate Stress (MPa)	% Elongation	% Reduction Of Area
Base Metal	254.33	400	28.2	61.57
Weld Metal	420.36	508.23	21.17	55.6

Table No. 4.3: Hardness across the Weld

Distance from weld center towards left (mm)	Hardness (HV5)		Distance from weld center towards right (mm)	Hardness (HV5)
0	221		0	221
1	221		1	232
2	210		2	221
3	232		3	221
4	221		4	210
5	168		5	210
6	168		6	168
7	201		7	175
8	168		8	175
9	168		9	168
10	175		10	168
11	175		11	175
12	161		12	161
13	161		13	161
14	161		14	161

Table No. 4.4: Impact properties of C-Mn Steel and its Weld

		Test Temperature °C			
		-30	-15	0	10 (RT)
Energy absorbed in Joules	Base Metal	12	20	26	50
	Weld Metal	60	72	90	122

Table No. 4.5: Table for f(a/w) for FCGR Test C(T) Specimen

Crack Length (mm)	A/w	f(a/w)	Crack Length (mm)	a/w	f(a/w)
15.5	0.258	5.036	22.5	0.375	6.817
16.0	0.266	5.150	23.0	0.383	6.967
16.5	0.275	5.265	23.5	0.391	7.120
17.0	0.283	5.382	24.0	0.400	7.278
17.5	0.291	5.500	24.5	0.408	7.441
18.0	0.300	5.620	25.0	0.416	7.609
18.5	0.308	5.743	25.5	0.425	7.782
19.0	0.316	5.867	26.0	0.433	7.962
19.5	0.325	5.994	26.5	0.441	8.147
20.0	0.333	6.124	27.0	0.450	8.339
20.5	0.341	6.256	27.5	0.458	8.538
21.0	0.350	6.391	28.0	0.466	8.745
21.5	0.358	6.530	28.5	0.475	8.960
22.0	0.366	6.672	29.0	0.483	9.183

Table No. 4.6: Fatigue crack growth rate data for C-Mn Steel at R=0.1

Crack Length (mm)	No of Cycles	ΔK MPa√m	da/dN m/cycle $X10^{-7}$		Crack Length (mm)	No Of Cycles	ΔK MPa√m	da/dN m/cycle $X10^{-7}$
15.5	0000	22.457	1.21		23.0	44930	31.054	3.14
16.0	4120	22.961	1.31		23.5	46520	31.741	2.76
16.5	7950	23.472	1.26		24.0	48330	32.448	2.67
17.0	11910	23.990	1.27		24.5	50200	33.177	2.84
17.5	15820	24.516	1.08		25.0	51960	33.930	3.57
18.0	20410	25.051	1.17		25.5	53360	34.707	4.0
18.5	24670	25.596	1.57		26.0	54610	35.510	4.34
19.0	27850	26.250	1.9		26.5	55760	36.342	3.96
19.5	30480	26.725	1.93		27.0	57020	37.204	4.46
20.0	33060	27.292	1.92		27.5	58140	38.099	4.8
20.5	35660	27.882	2.55		28.0	59180	39.028	5.31
21.0	37620	28.485	2.68		28.5	60120	39.994	5.88
21.5	39480	29.103	2.73		29.0	60970	40.999	6.66
22.0	41370	29.736	2.71		29.5	61590	42.047	7.02
22.5	43150	30.386	2.8		30.0	72280	43.139	7.54

Table No. 4.7: Fatigue crack growth rate data for C-Mn Steel at R=0.3

Crack Length (mm)	No of Cycles	ΔK MPa√m	da/dN m/cycle $X10^{-7}$		Crack Length (mm)	No Of Cycles	ΔK MPa√m	da/dN m/cycle $X10^{-7}$
15.5	0000	1.288	0.714		23.0	68470	1.428	1.78
16.0	6900	1.297	0.724		23.5	71090	1.438	1.905
16.5	13190	1.307	0.794		24.0	73540	1.447	2.04
17.0	19410	1.316	0.795		24.5	75670	1.457	2.34
17.5	25100	1.326	0.89		25.0	77990	1.467	2.15
18.0	30100	1.335	1.0		25.5	79980	1.477	2.51
18.5	35330	1.344	0.955		26.0	81880	1.486	2.63
19.0	39990	1.354	1.07		26.5	83650	1.497	2.82
19.5	44340	1.363	1.15		27.0	87010	1.507	3.16
20.0	48310	1.372	1.26		27.5	90370	1.517	3.16
20.5	52190	1.382	1.29		28.0	93370	1.528	3.54
21.0	56070	1.391	1.29		28.5	96040	1.538	3.98
21.5	59450	1.4	1.48		29.0	98840	1.549	3.8
22.0	62460	1.409	1.66		29.5	101280	1.560	4.36
22.5	65670	1.419	1.56		30.0	103550	1.572	4.688

Table No. 4.8: Fatigue crack growth rate data for C-Mn Steel Weld at R=0.1

Crack Length (mm)	No of Cycles	ΔK MPa√m	da/dN m/cycle $X10^{-7}$		Crack Length (mm)	No of Cycles	ΔK MPa√m	da/dN m/cycle $X10^{-7}$
15.5	0000	1.438	0.544		23.0	71170	1.579	2.133
16.0	8360	1.448	0.598		23.5	73300	1.588	2.342
16.5	15980	1.457	0.656		24.0	75240	1.598	2.571
17.0	22950	1.467	0.718		24.5	77230	1.608	2.510
17.5	29290	1.476	0.79		25.0	78810	1.617	3.160
18.0	35050	1.485	0.865		25.5	80250	1.627	3.467
18.5	40330	1.495	0.946		26.0	81580	1.637	3.767
19.0	45110	1.504	1.047		26.5	82780	1.647	4.173
19.5	49470	1.514	1.12		27.0	83870	1.657	4.592
20.0	53540	1.523	1.25		27.5	84850	1.668	5.071
20.5	56840	1.532	.1513		28.0	85740	1.678	5.620
21.0	60520	1.541	1.358		28.5	86540	1.699	6.220
21.5	63520	1.551	1.66		29.0	87260	1.710	6.918
22.0	66330	1560	1.78		29.5	87910	1.722	7.690
22.5	68830	1.569	1.99		30.0	88490	1.733	8.577

Table No. 4. 9: Fatigue crack growth rate data for C-Mn Steel Weld at R=0.3

Crack Length (mm)	No of Cycles	ΔK MPa√m	da/dN m/cycle $X10^{-7}$		Crack Length (mm)	No of Cycles	ΔK MPa√m	da/dN m/cycle $X10^{-7}$
15.5	0000	27.448	0.544		23.0	71170	37.955	2.135
16.0	8360	28.064	0.598		23.5	73300	38.795	2.342
16.5	15980	28.688	0.656		24.0	75240	39.659	2.570
17.0	22950	29.321	0.718		24.5	77230	40.551	2.516
17.5	29290	29.964	0.79		25.0	78810	41.473	3.163
18.0	53050	30.618	0.865		25.5	80250	42.412	3.467
18.5	40330	31.283	0.946		26.0	81580	43.402	3.767
19.0	45110	31.961	1.047		26.5	82780	44.418	4.171
19.5	49570	32.652	1.120		27.0	83870	45.472	4.593
20.0	53540	33.357	1.25		27.5	84850	46.566	5.072
20.5	56840	34.078	1.513		28.0	85740	47.701	5.623
21.0	60520	34.815	1.358		28.5	86540	48.882	6.227
21.5	63520	35.571	1.66		29.0	87260	50.115	6.918
22.0	66330	36.345	1.78		29.5	87910	51.391	7.690
22.5	68830	37.139	1.99		30.0	88490	52.726	8.576

Table No. 4.10 Summary of fatigue crack growth rate tests results

Material	Stress Ratio (R)	Paris Constants		ΔK_{th}
		m	c	
Base Metal	0.1	2.6921	$2.63X10^{-11}$	1.64
	0.3	2.9646	$1.03X10^{-11}$	2.15
Weld Metal	0.1	4.2203	$4.62X10^{-14}$	6.15
	0.3	4.6565	$9.48X10^{-15}$	7.31

Table No. 4.11 Initial and final crack length of specimens used for Jic test of CMn Steel

Readings	B-1		B-2		B-3		B-4		B-5		B-6	
	(a_o)	(a_f)	(a_o)	(a_f)	$(a)_o$	$(a)_f$	$(a)_o$	$(a)_f$	$(a)_o$	$(a)_f$	$(a)_o$	$(a)_f$
1	23.21	23.50	23.88	24.23	23.80	25.63	25.24	25.79	23.90	25.17	24.07	25.40
2	23.74	24.94	25.11	25.76	24.78	26.25	25.47	26.92	25.47	26.94	24.82	26.68
3	25.09	25.37	24.67	25.62	25.23	26.92	25.88	27.28	25.67	27.64	25.98	28.98
4	25.31	25.67	25.14	25.89	25.87	27.18	25.69	26.99	25.54	28.35	26.36	28.32
5	25.15	25.41	24.94	25.48	25.66	27.47	25.05	26.49	25.71	28.25	26.36	27.94
6	25.16	25.60	24.83	25.61	25.81	26.88	24.82	25.43	25.55	27.0	26.06	29.16
7	25.48	25.67	25.08	25.32	25.25	26.49	24.62	25.78	24.98	26.94	25.84	28.56
8	24.12	24.08	24.73	25.78	24.95	26.31	24.95	25.84	24.78	27.14	24.88	27.26
9	24.01	24.56	24.54	25.12	24.67	26.34	24.54	25.34	24.57	26.73	24.08	26.93
Average	24.58	25.06	24.76	25.42	25.11	26.68	25.14	26.20	25.132	27.13	25.38	27.69

Table No. 4.12 Initial and final crack length of specimens used for Jic test of CMn Steel Weld

Readings	W-1		W-2		W-3		W-4		W-5		W-6		W-7		W-8	
	a_o	a_f	a_o	a_f	a_o	a_f	a_o	a_f	a_o	a_f	a_o	a_f	a_o	a_f	a_o	a_f
1	24.63	24.94	23.05	23.65	22.83	23.75	24.24	26.02	24.04	26.38	24.09	26.14	24.09	25.78	25.63	27.39
2	25.96	26.75	23.58	23.92	23.73	26.02	25.67	27.01	25.27	26.91	24.54	26.98	25.20	27.27	26.62	29.90
3	26.19	26.34	23.88	24.40	23.84	25.77	26.01	26.08	25.19	26.52	25.67	26.46	24.59	26.76	26.63	29.79
4	26.05	26.25	24.34	25.72	24.84	25.81	25.61	26.52	24.55	26.09	25.31	26.73	25.01	27.20	26.53	29.25
5	25.45	25.85	24.54	24.75	24.95	25.75	24.88	26.78	24.08	25.86	24.74	26.82	25.14	27.20	26.09	29.19
6	25.27	25.93	24.28	24.64	24.85	25.97	24.74	26.0	23.69	25.19	24.77	27.31	25.35	27.06	25.60	29.40
7	25.24	26.14	24.68	25.84	24.14	24.87	24.56	25.71	23.78	25.13	24.25	26.19	25.41	26.92	25.54	30.59
8	24.80	25.73	24.42	25.14	23.94	24.52	24.44	25.81	23.92	26.03	25.38	26.35	25.08	26.97	25.38	28.82
9	24.43	25.13	23.14	24.25	23.62	24.36	24.12	25.28	24.22	26.34	24.14	26.25	24.34	26.83	24.22	28.65
Average	25.33	25.89	24.00	24.70	24.08	25.20	24.92	26.13	24.31	26.05	24.65	26.58	24.91	26.88	25.79	29.22

Table No. 4.13 Summary of J_{1C} tests results of Base metal

Specimen No.	Δa_p mm	J_{pl} KJ/m²	J_{el} KJ/m²	J KJ/m²
B-1	0.477	180.0	19.07	199.07
B-2	0.655	214.8	18.24	233.04
B-3	1.06	293.7	19.92	313.62
B-4	1.568	367.2	18.85	386.05
B-5	1.996	433.0	17.42	450.42
B-6	2.309	490.5	16.27	405.77
J_{1C}= 210 KJ/m²				

Table No. 4.14 Summary of Jic tests results of CMn Steel Weld

Specimen No.	Δa_p mm	J_{pl} KJ/m²	J_{el} KJ/m²	J KJ/m²
W-1	0.560	247.33	32.68	280.01
W-2	0.701	279.82	31.72	311.54
W-3	1.121	305.90	24.14	330.04
W-4	1.216	390.53	36.48	427.01
W-5	1.746	404.54	27.42	431.96
W-6	1.927	525.32	36.56	561.88
W-7	1.975	561.31	35.21	596.52
W-8	3.430	676.60	33.47	710.07
				J_{IC}= 270 KJ/m²

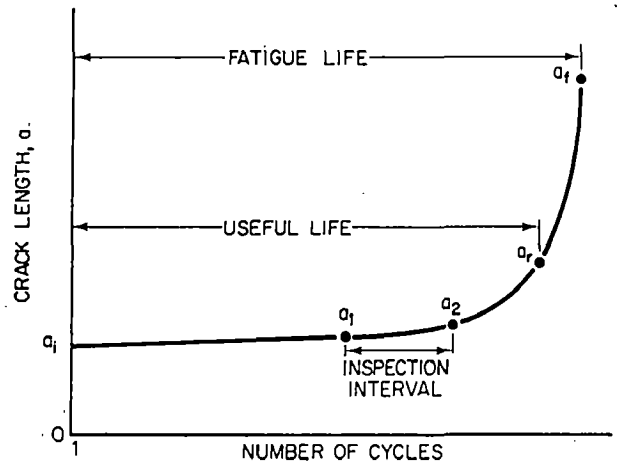

Fig. 2.1 Schematic representation of fatigue crack growth curve

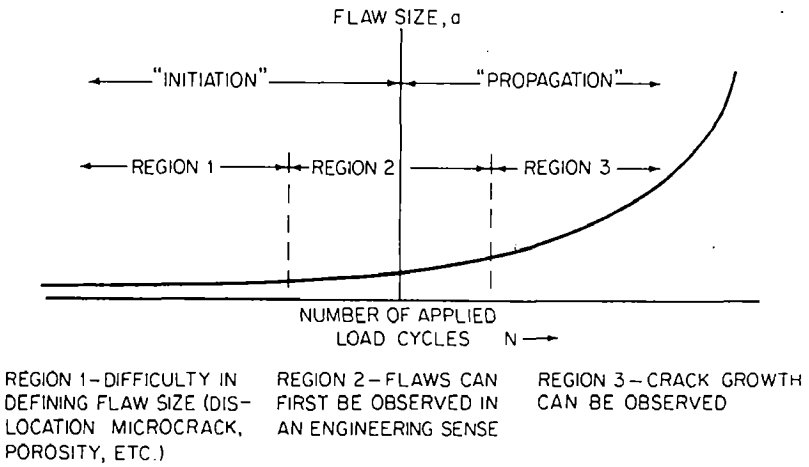

Fig. 2.2 Schematic showing relationship between "initiation" life and"propagation"life.

G10330.

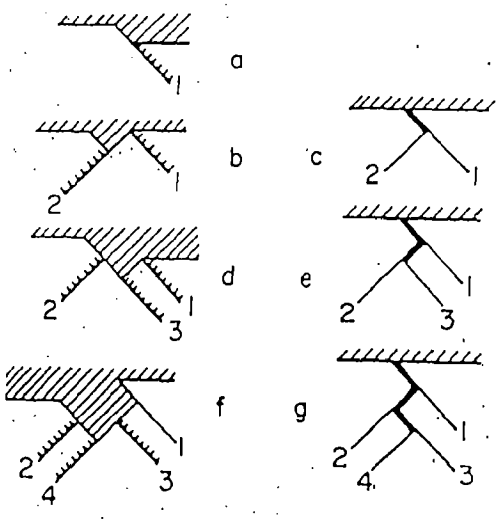

Fig. 2.3 Neuman model for the formation of crack by coarse slip.

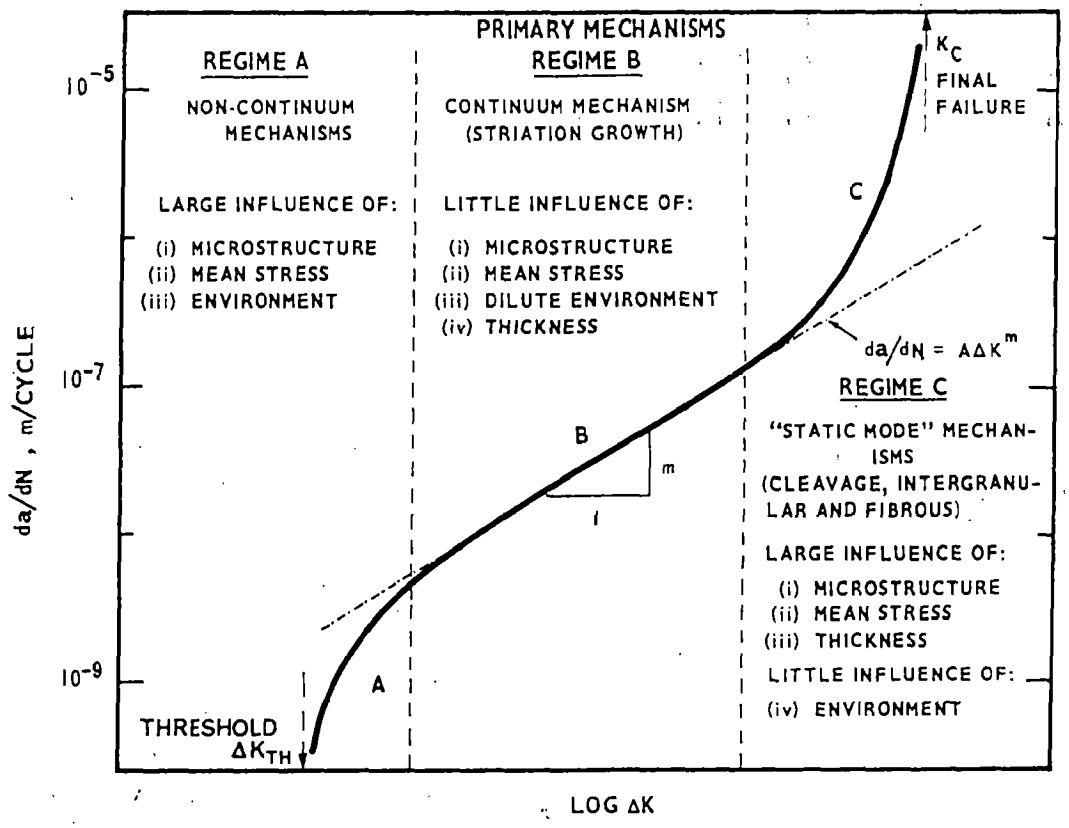

FIG.2.4. Summary diagram showing the primary fracture mechanisms associated with the 'sigmoidal' variation of fatigue crack propagation rate da/dN with alternating stress intensity ΔK. ΔK_{TH} is the threshold stress intensity for crack growth and K_C the stress intensity at final failure (terminal K).

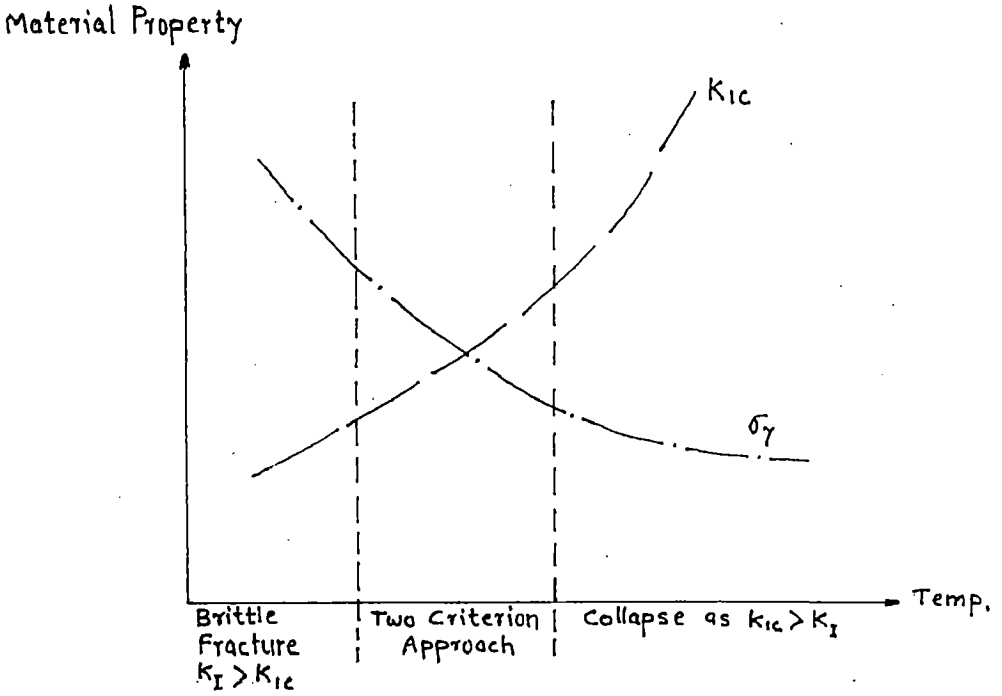

Fig. 2.5 Schematic representation of the condition for the brittle and ductile fracture

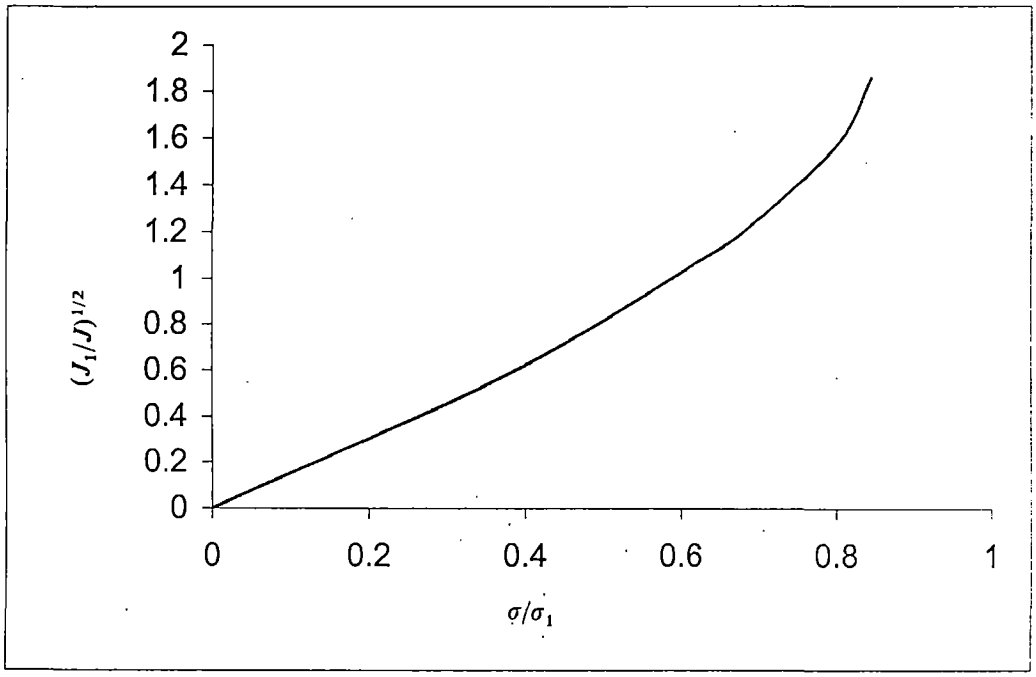

Fig. 2.6 Typical $(J/J_1)^{1/2}$ against (σ/σ_1) curve.

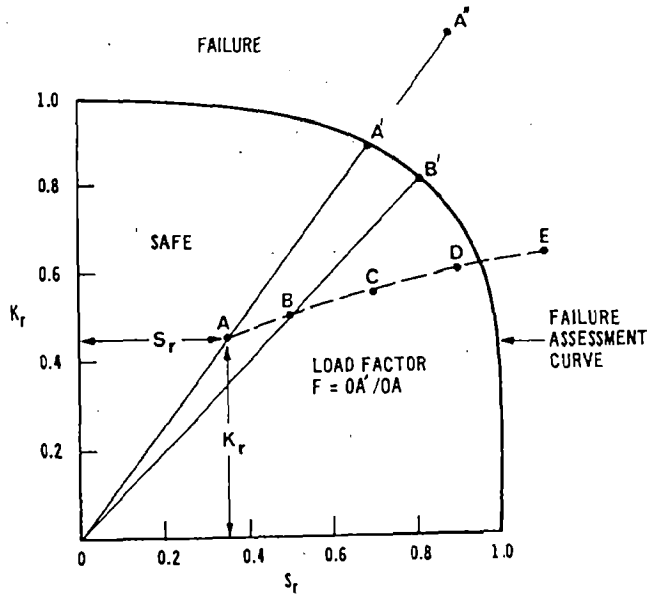

Fig. 2.7 The failure assessment diagram based upon semi-empirical modification to the strip yielding model.

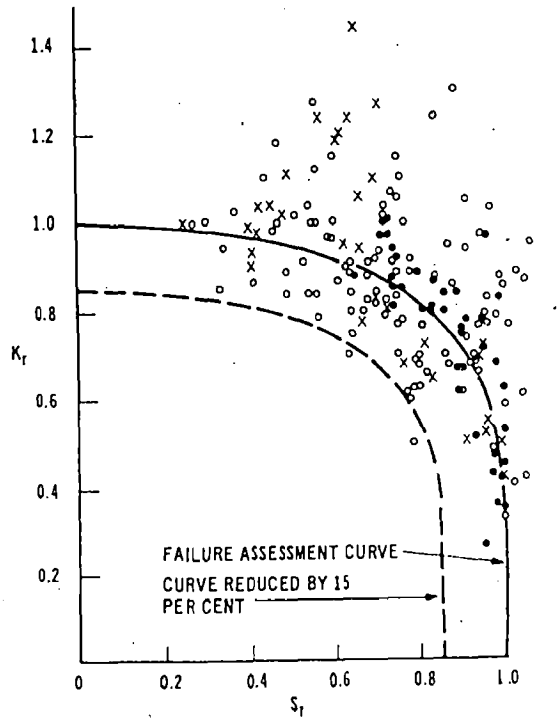

Fig. 2.8 Experimentation validation of the failure assessment diagram.

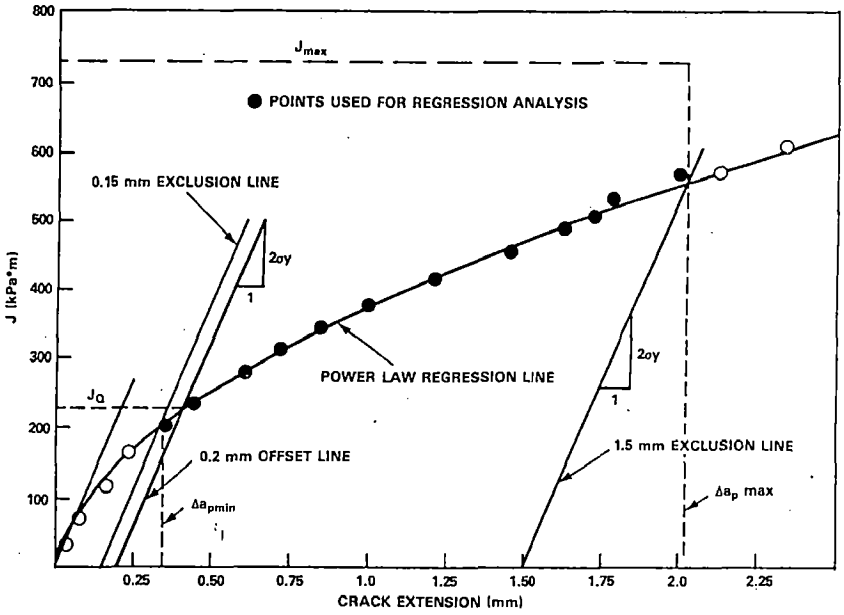

Fig. 2.9 Definition for data qualification for J_{IC} test.

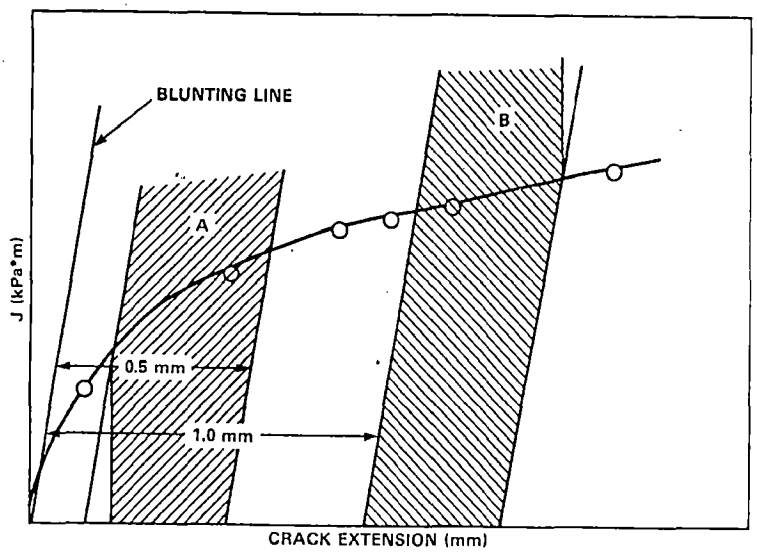

Fig. 2.10 Definition of regions for data point spacing.

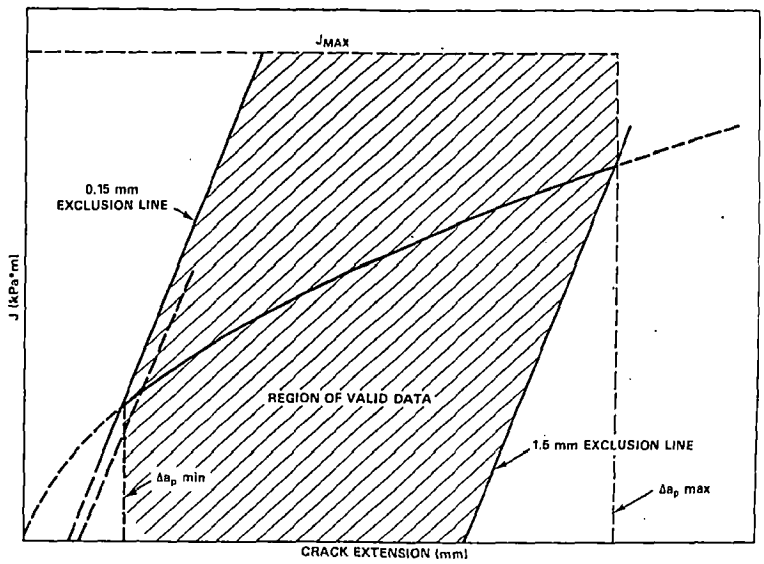

Fig. 2.11 Definition of region of valid data.

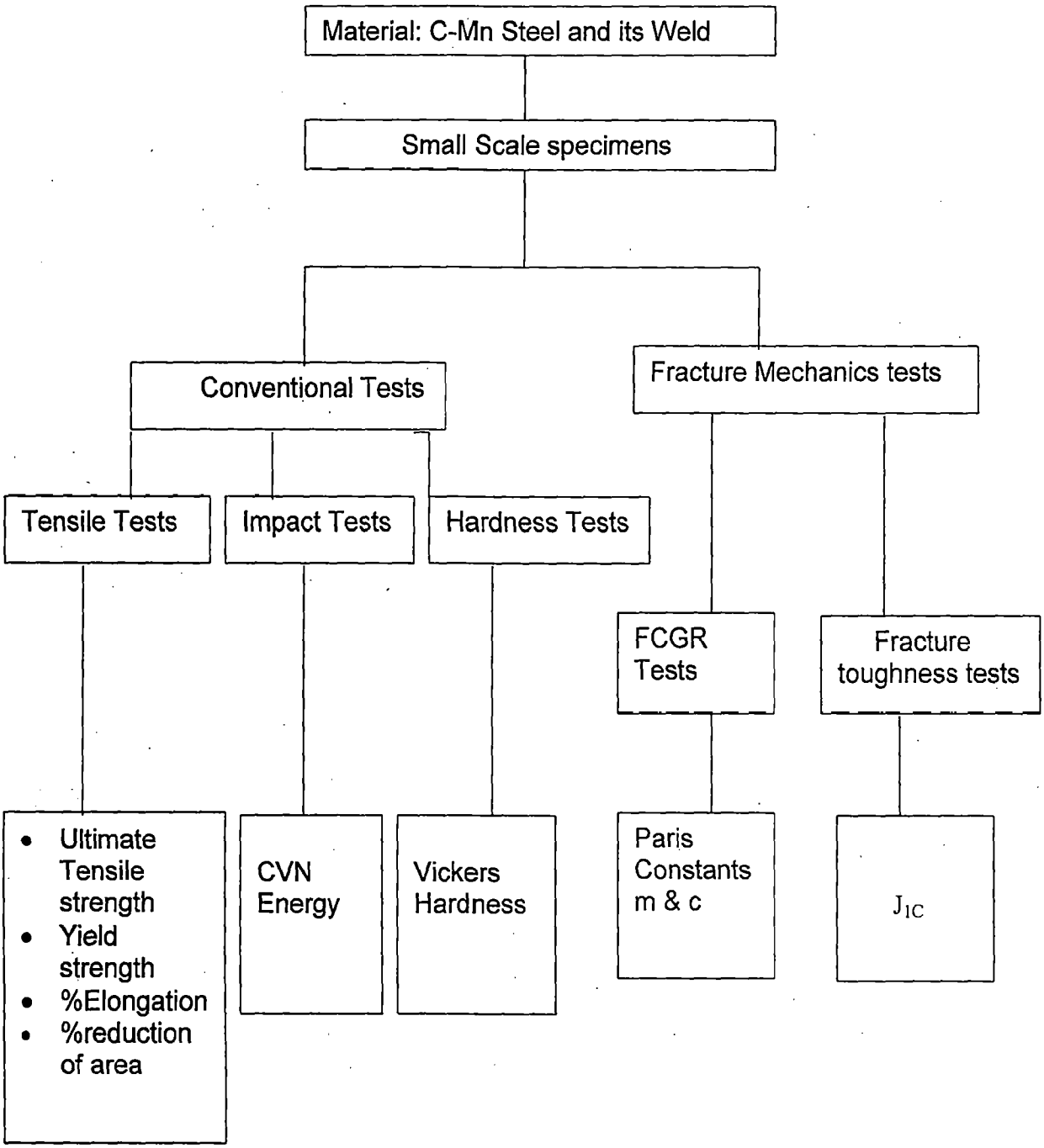

Fig. 3.1: Schematic representation of experimental plan

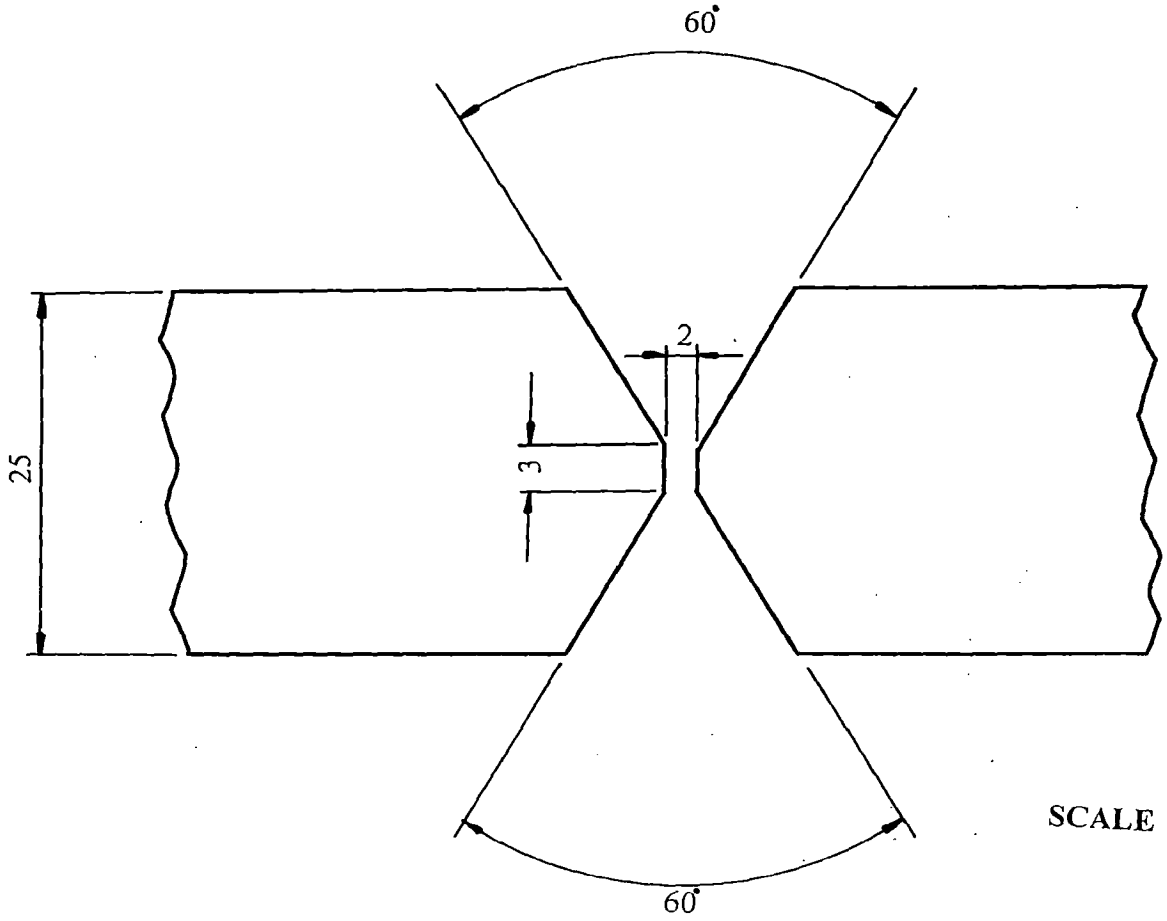

Fig. 3.2 A complete detail of Groove Design.

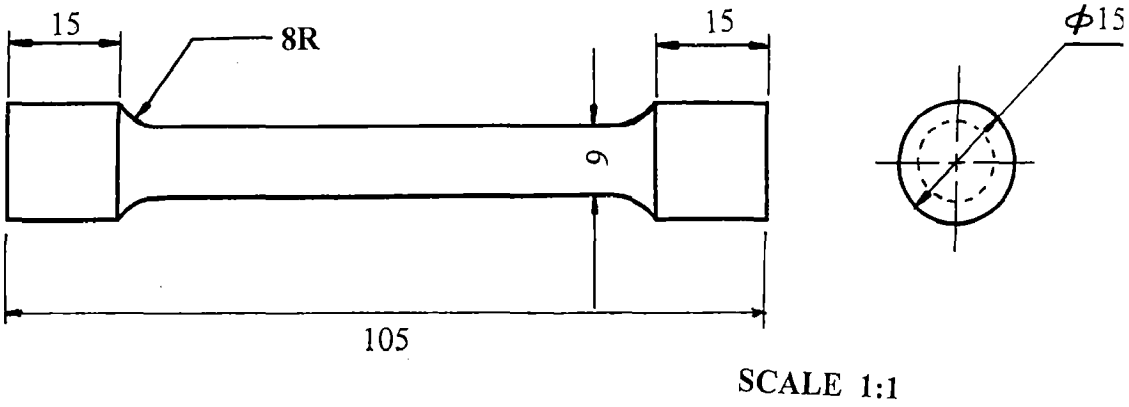

Fig. 3.3 Tensile Test Specimen.

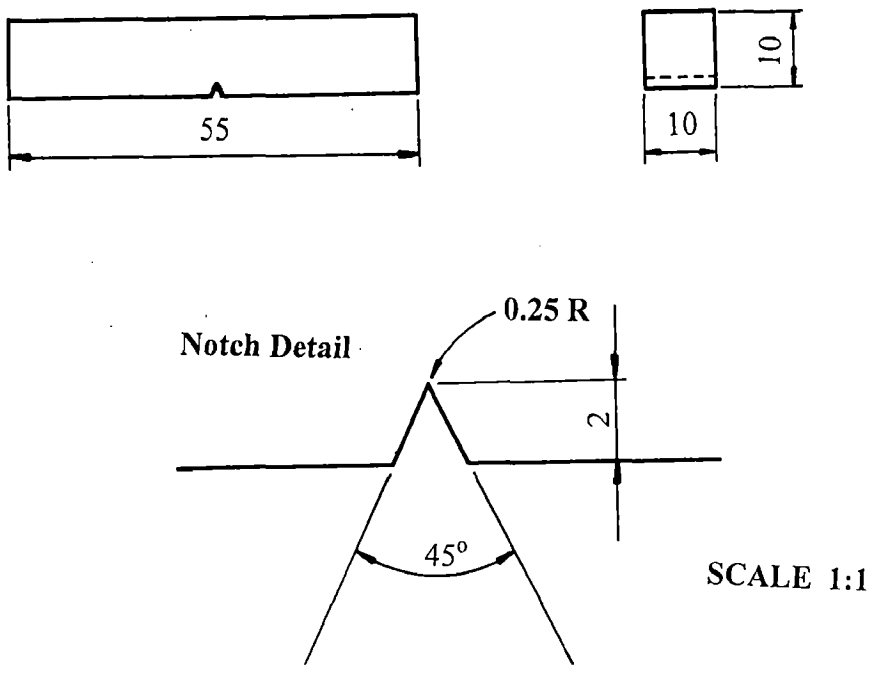

Fig. 3.4 Charpy V-notch Impact Test Specimen.

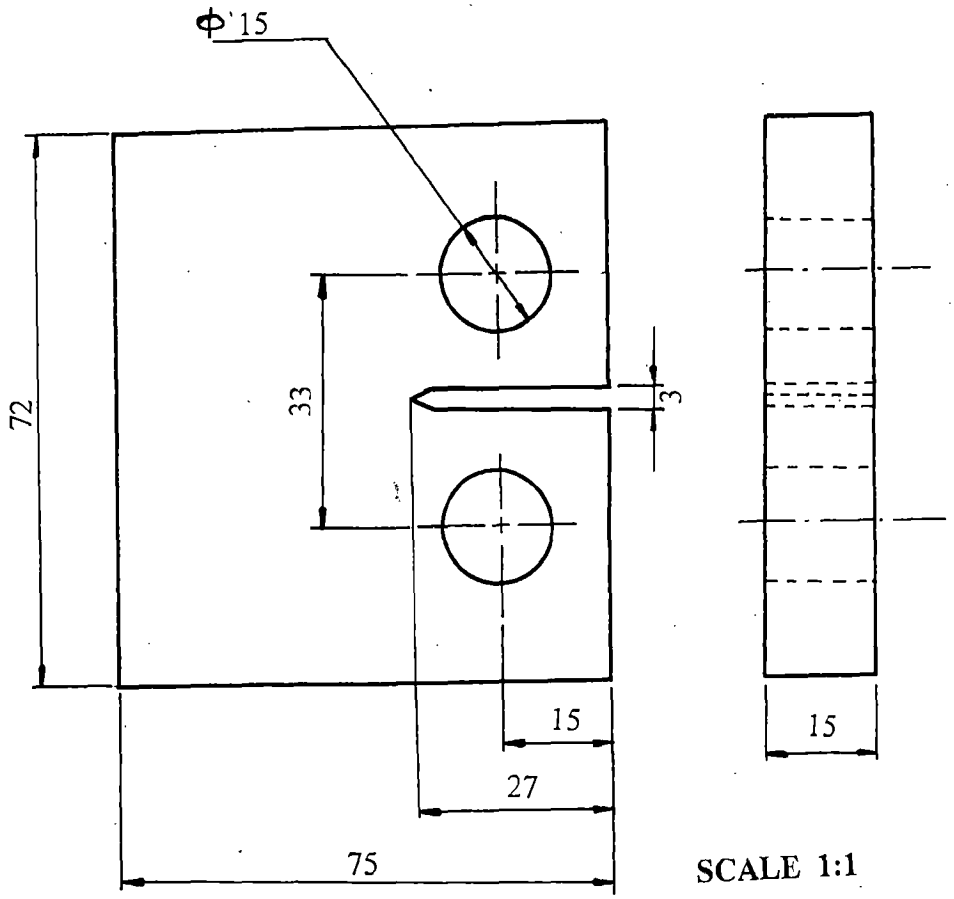

Fig.3.5 C(T) Specimen for Crack Growth Rate Test.

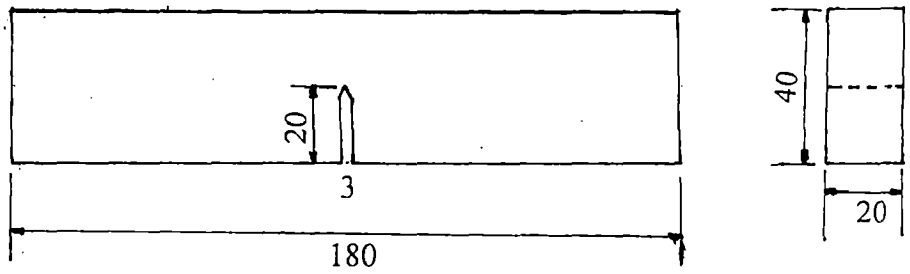

Fig. 3.6 TPB Specimen for Fracture Toughness (J_{IC}) Test.

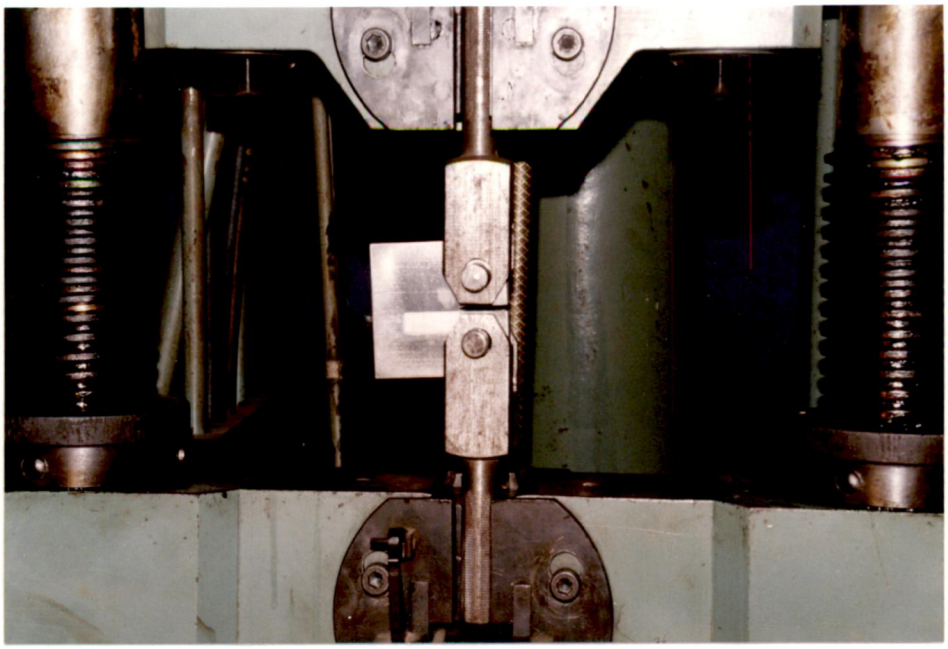

Fig. 3.7 Photograph showing FCGR test arrengement.

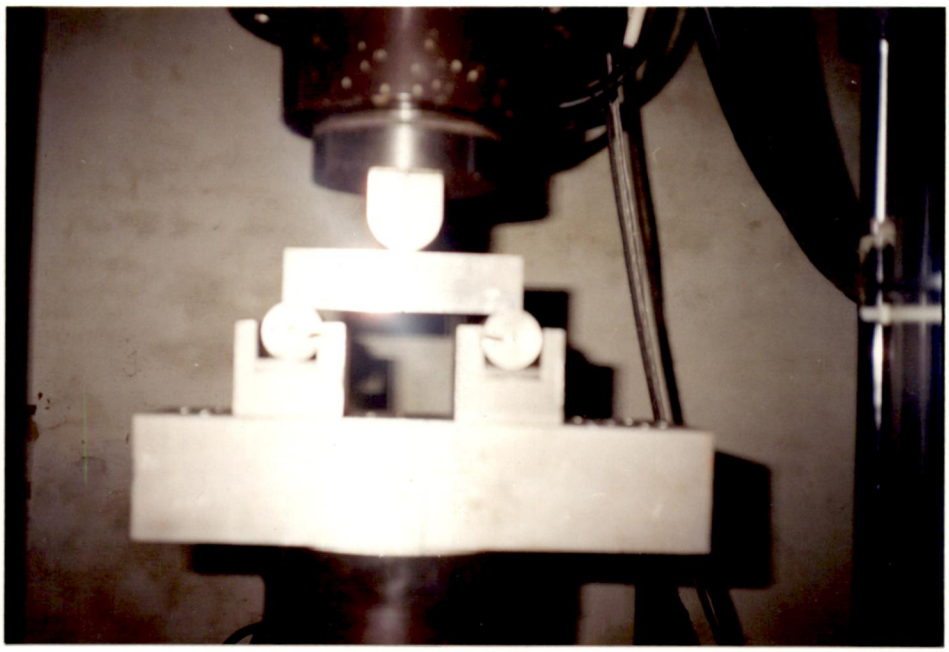

Fig. 3.8 Photograph showing (J_{IC}) test arrengement.

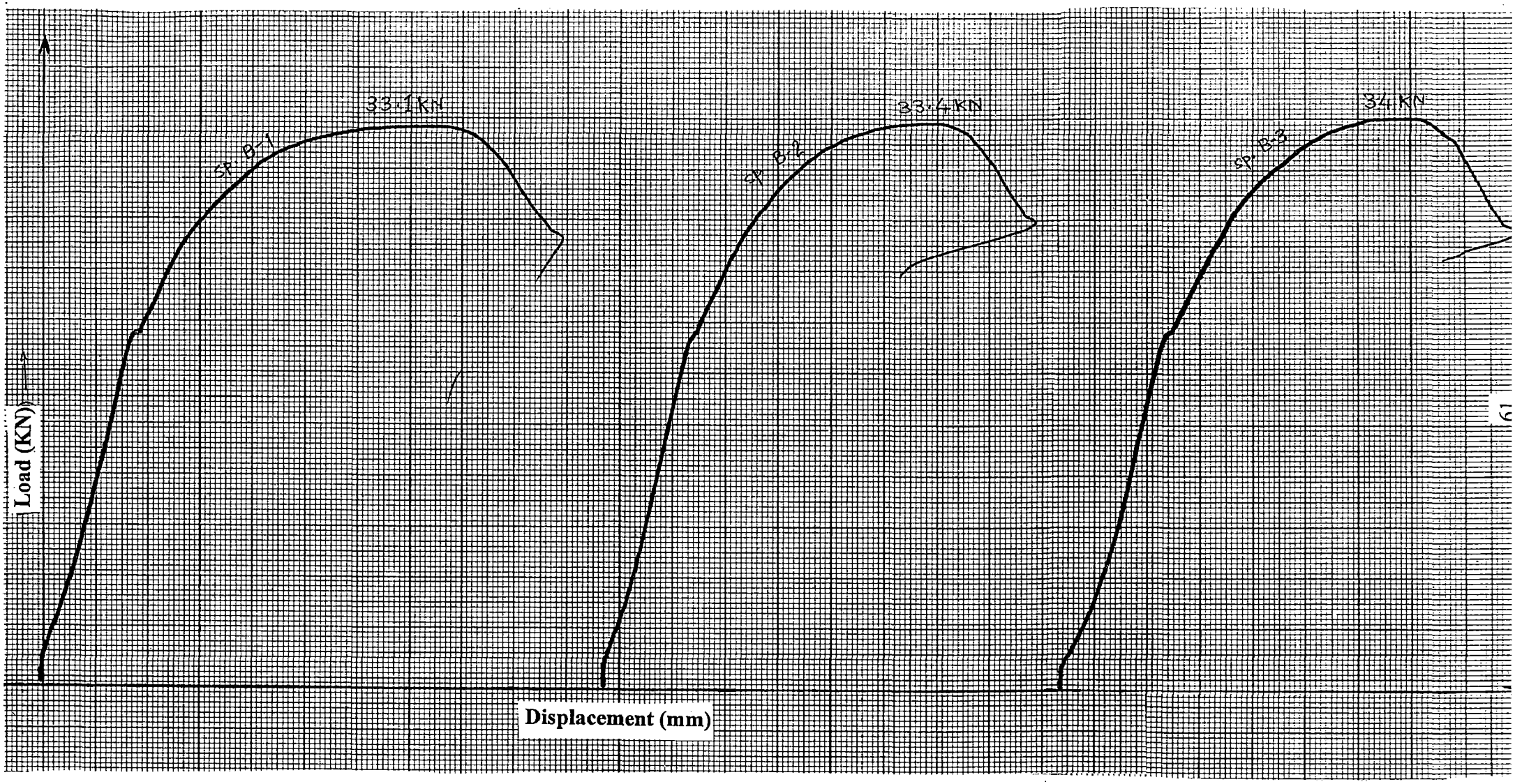

Fig. 4.1 Load displacement(Tensile test) curve for C-Mn Steel.

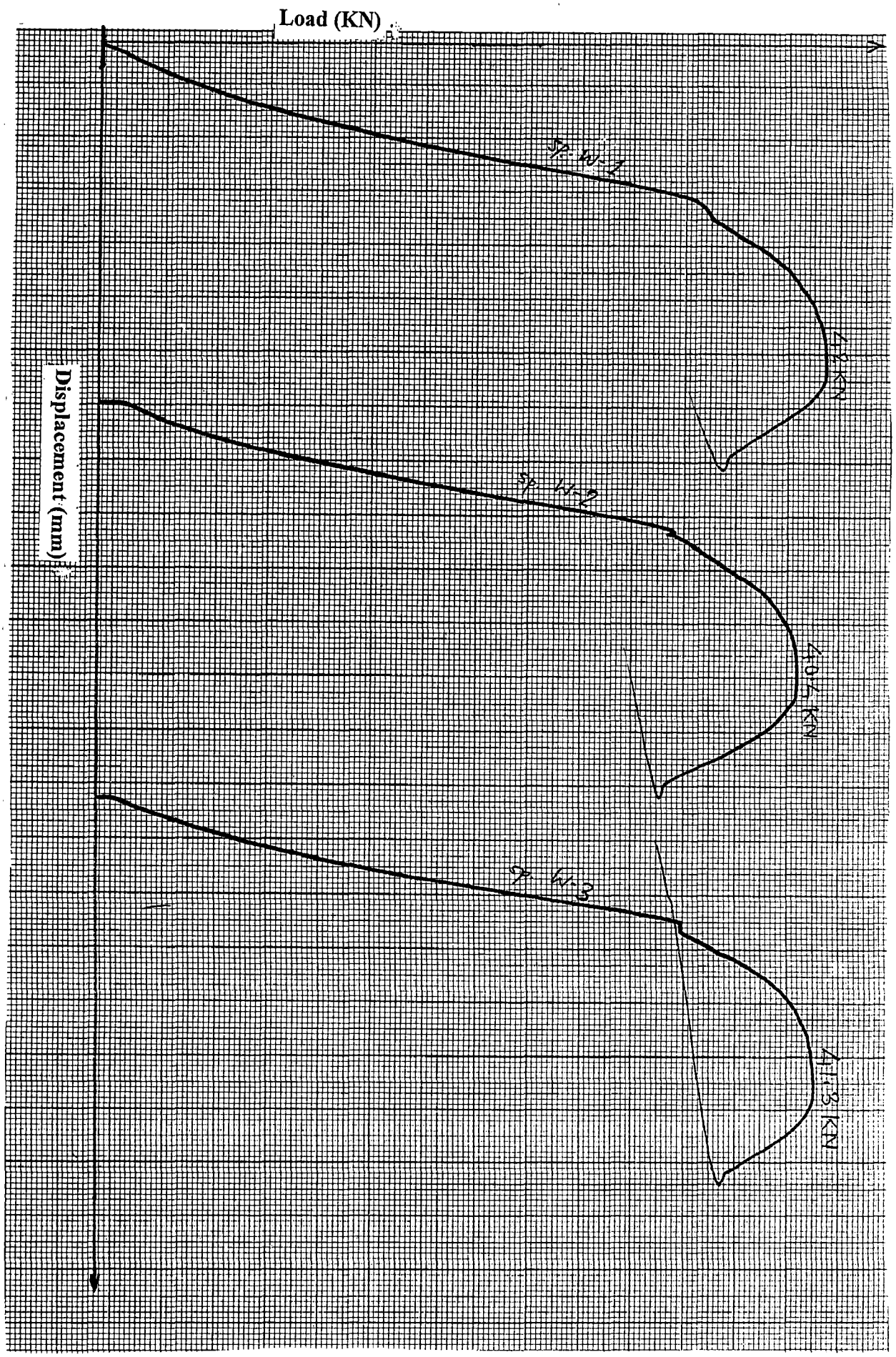

Fig. 4.2 Load displacement(Tensile test) curve for C-Mn Steel Weld.

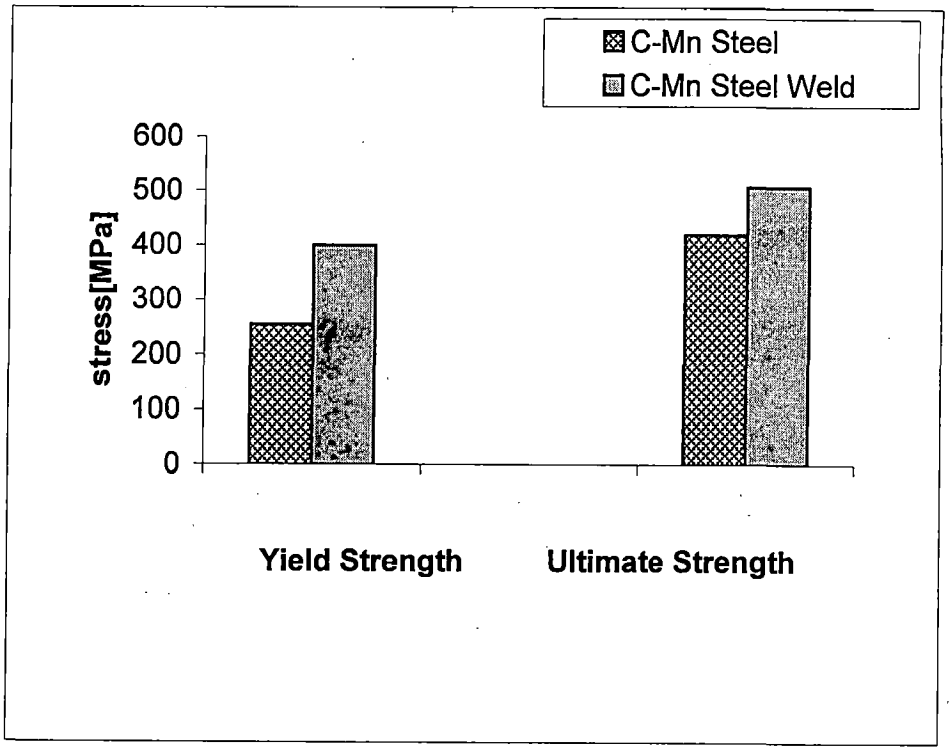

Fig. 4.3 Schematic representation of Yield Strength and Ultimate Strength of C-Mn Steel and its Weld.

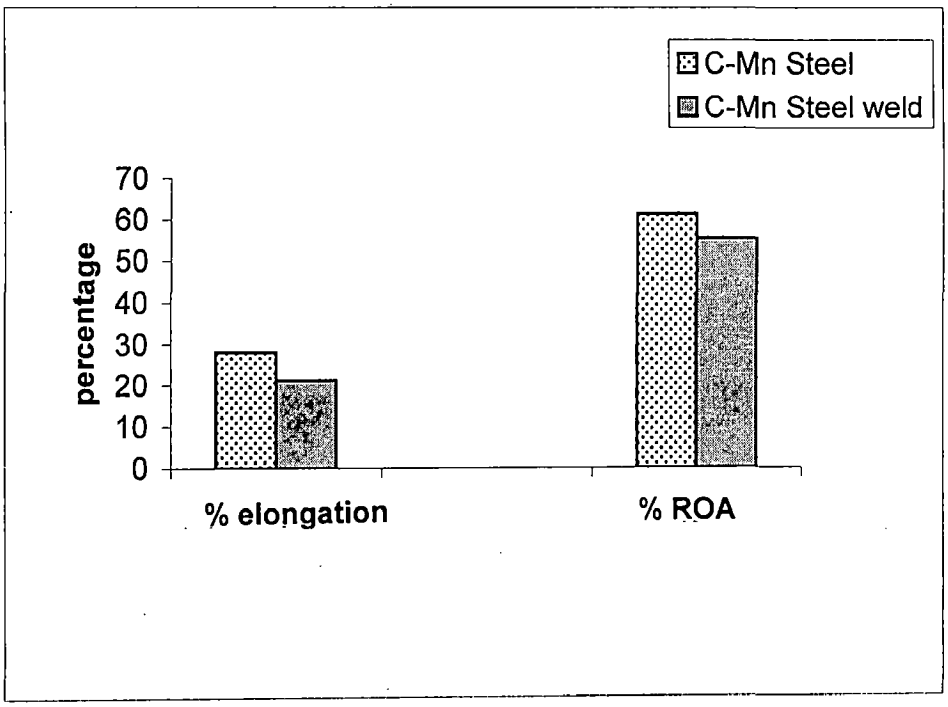

Fig. 4.4 Schematic representation of % Elongation and % Reduction of Area of C-Mn Steel

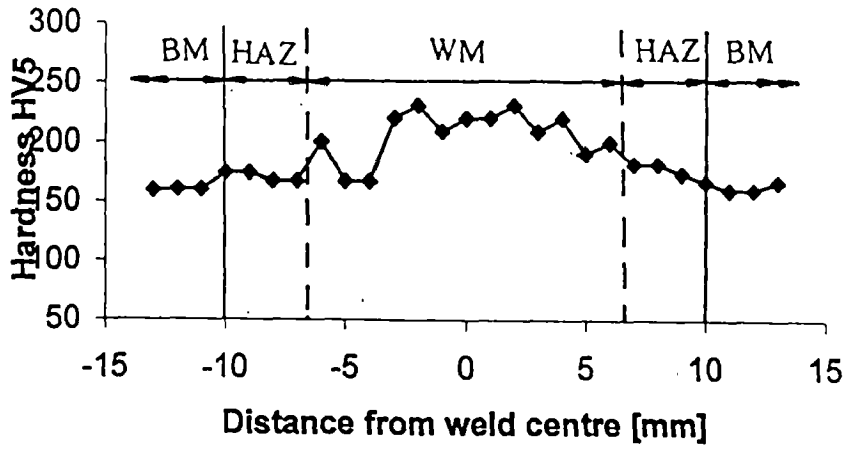

Fig. 4.5: schematic representation of hardness distribution across the weld

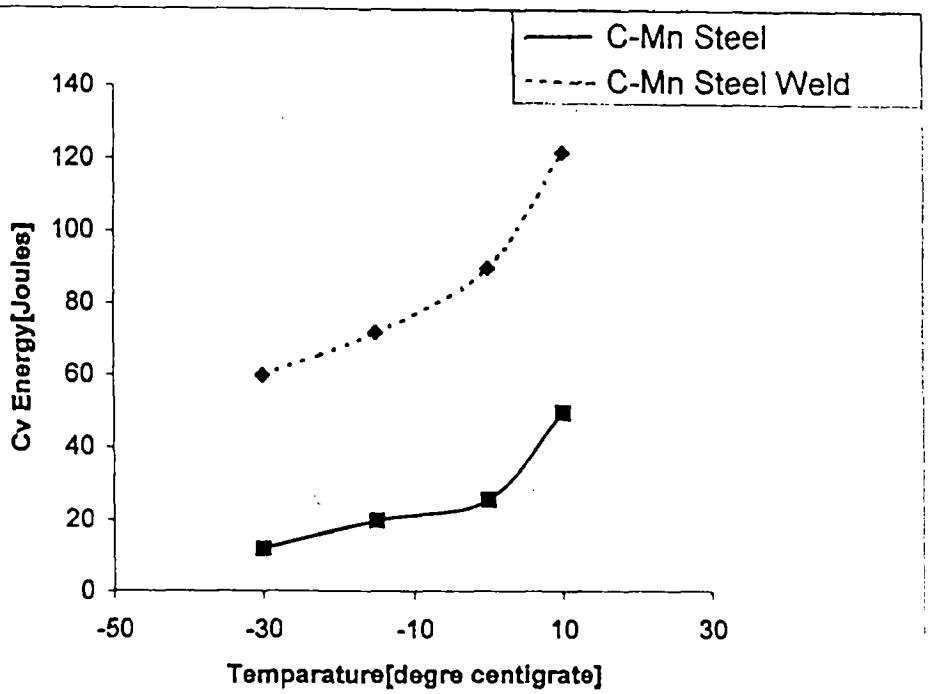

Fig. 4.6: Schematic representation of Toughness of C-Mn Steel & its weld

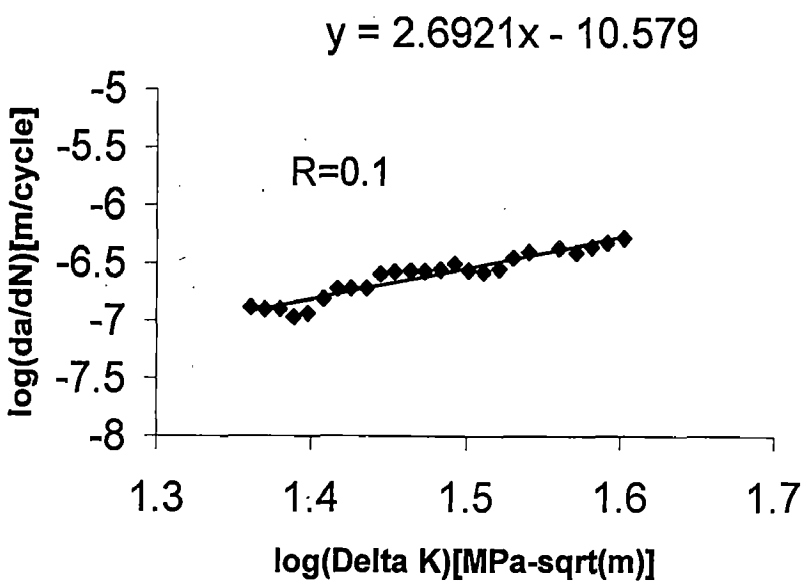

Fig. 4.7 da/dN Vs. ΔK plot of C-Mn Steel at R = 0.1 on log-log scale.

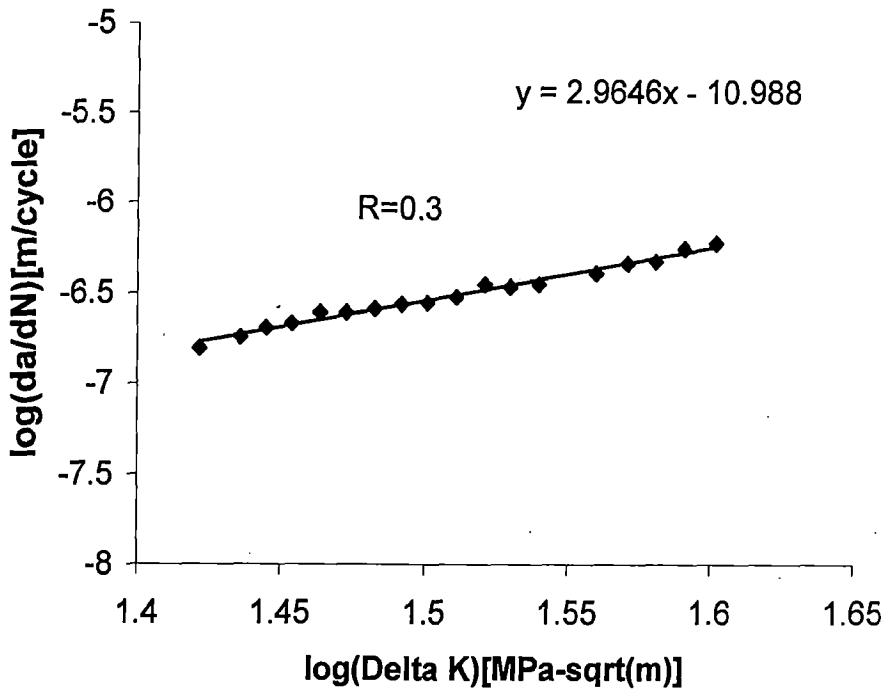

Fig. 4.8 da/dN Vs. ΔK plot of C-Mn Steel at R = 0.3 on log-log scale.

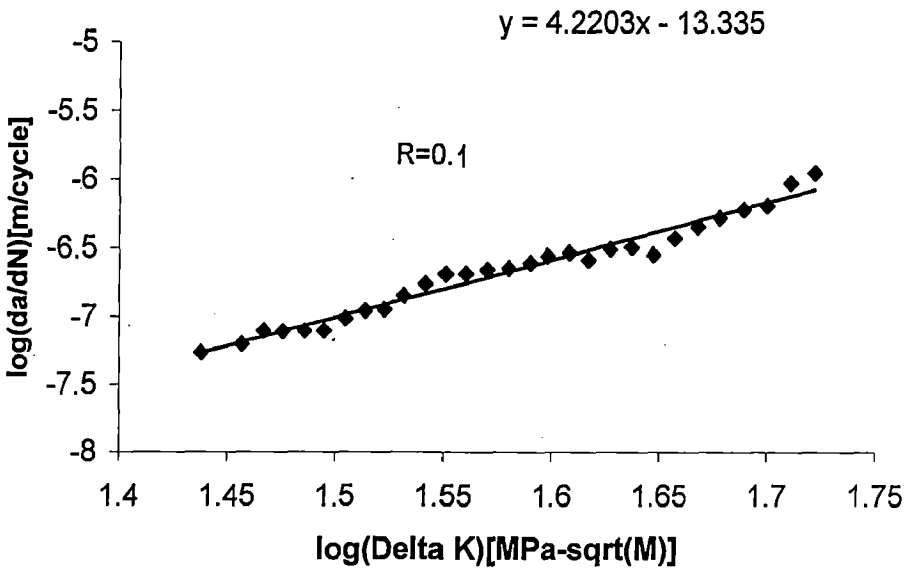

Fig. 4.9 da/dN Vs. ΔK plot of C-Mn Steel Weld at R = 0.1 on log-log scale.

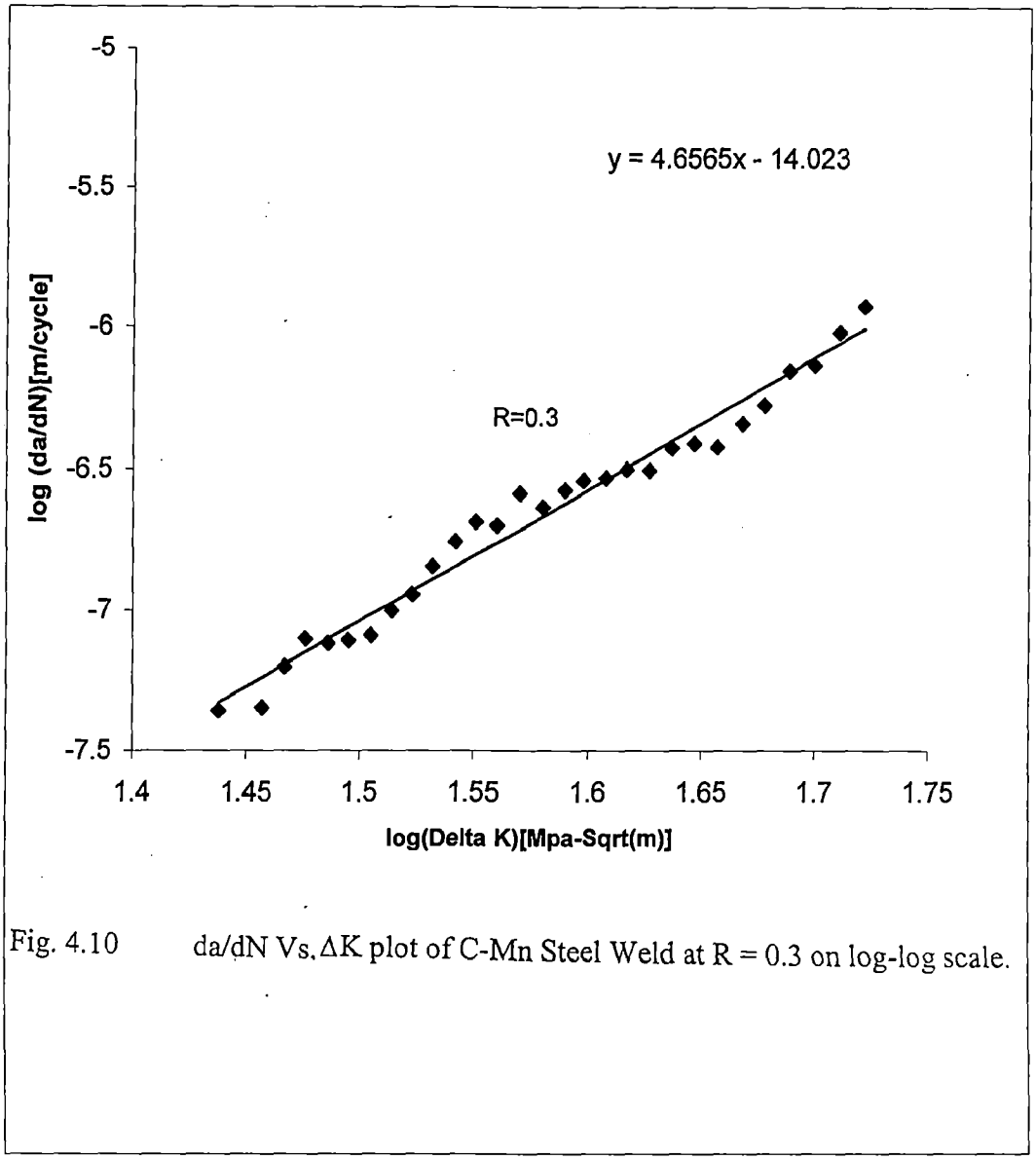

Fig. 4.10 da/dN Vs. ΔK plot of C-Mn Steel Weld at R = 0.3 on log-log scale.

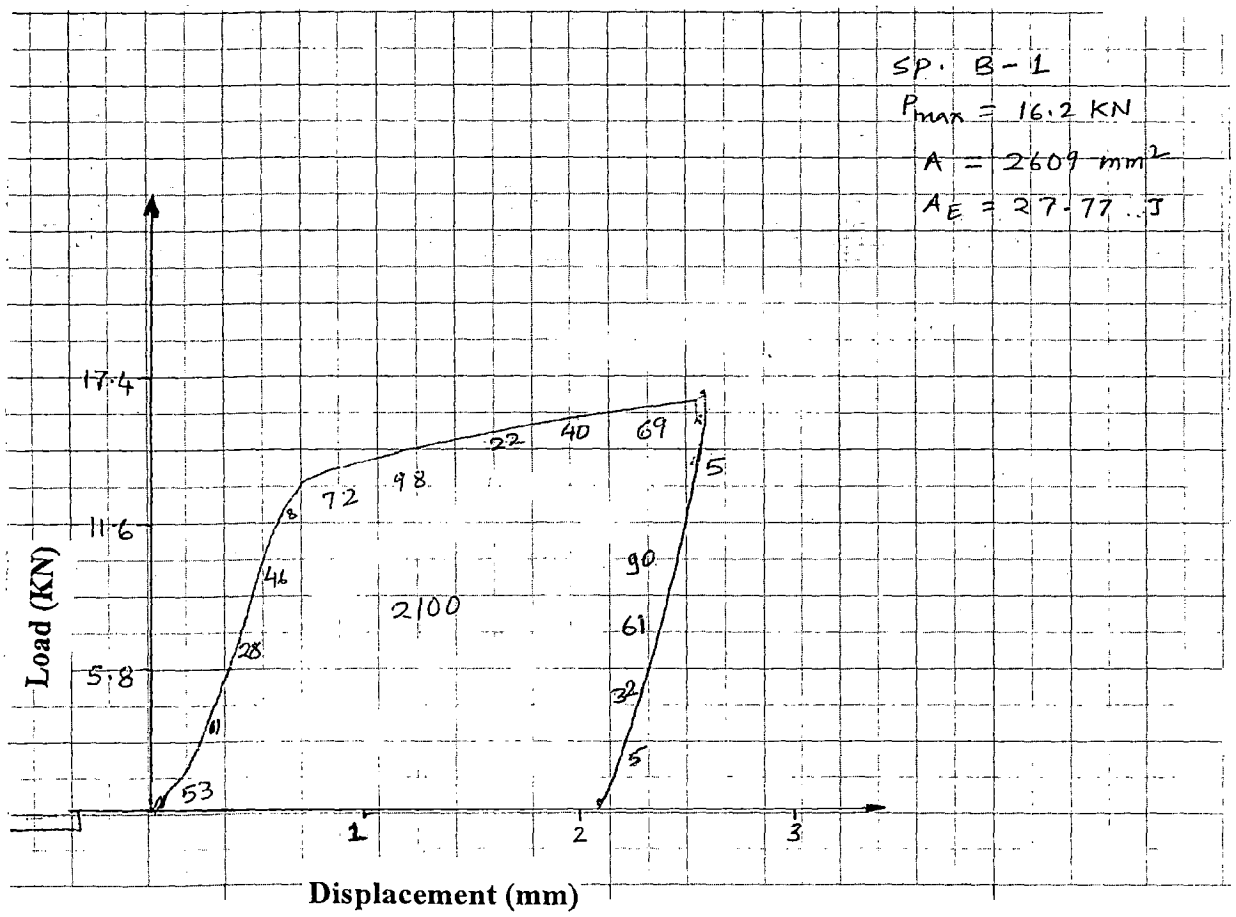

Fig. 4.11 Load displacement curve for base metal specimen B-1 of J_{IC} test.

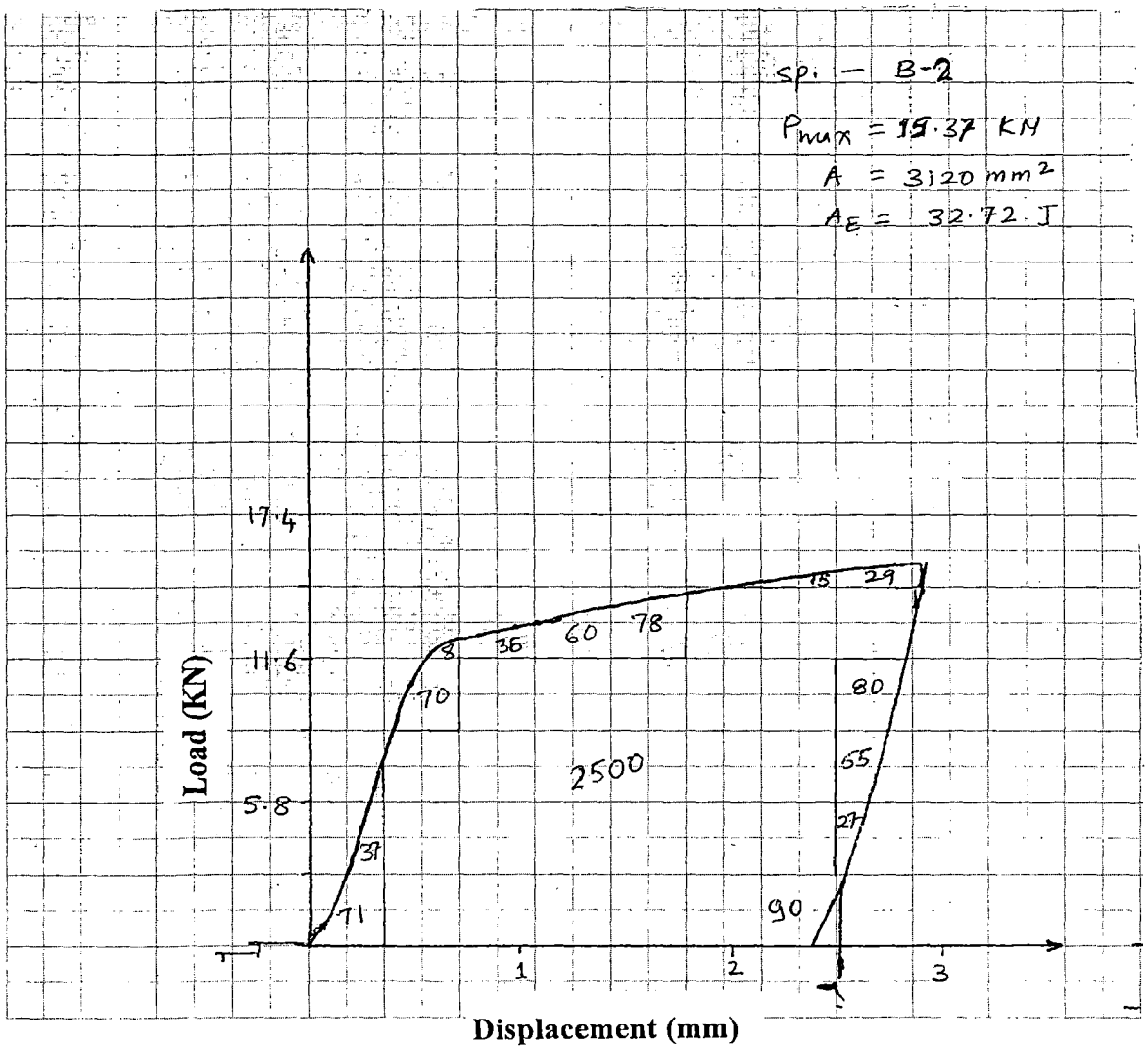

Fig. 4.12 Load displacement curve for base metal specimen B-2 of J_{IC} test.

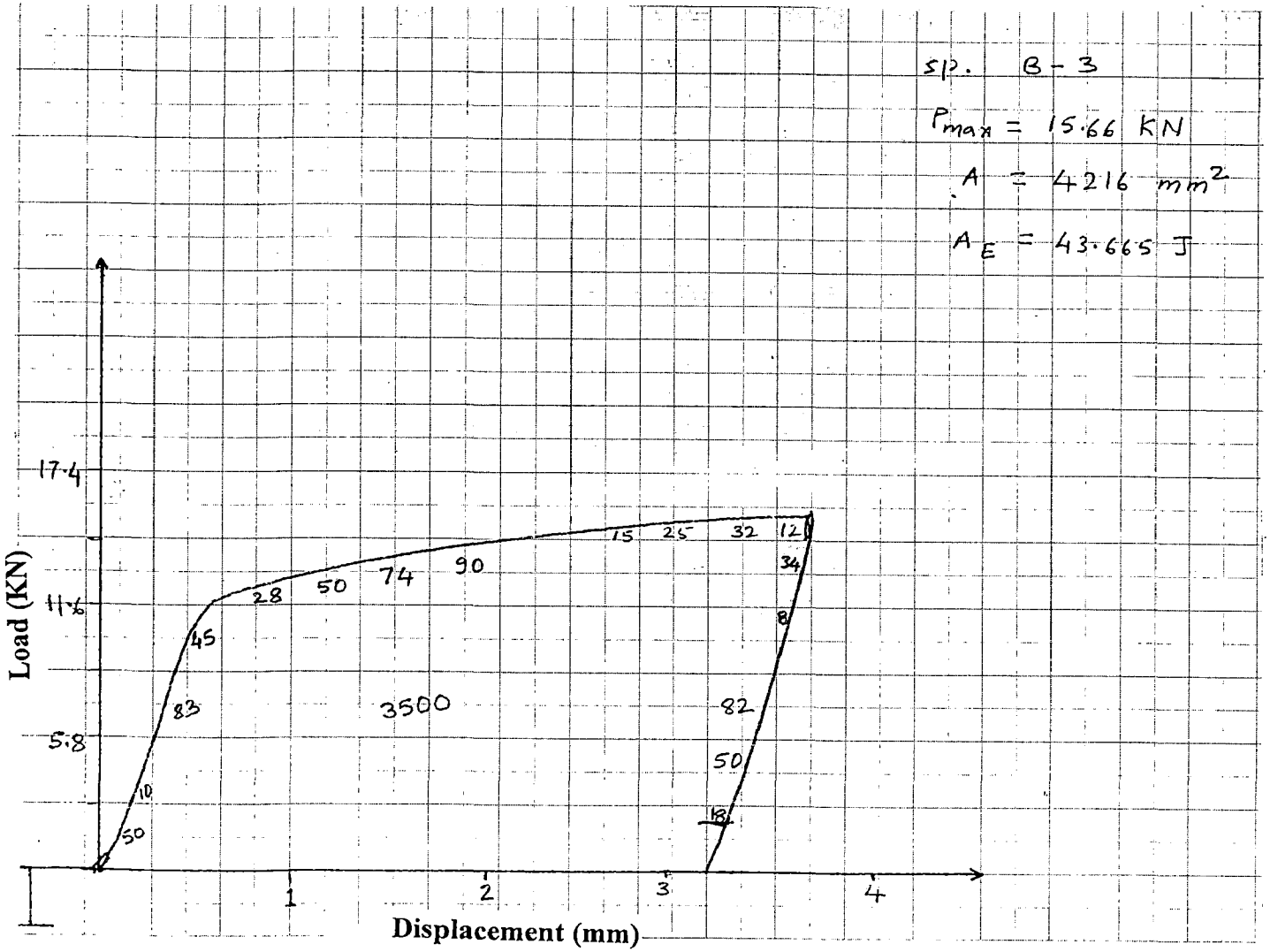

Fig. 4.13 Load displacement curve for base metal specimen B-3 of J_{1C} test.

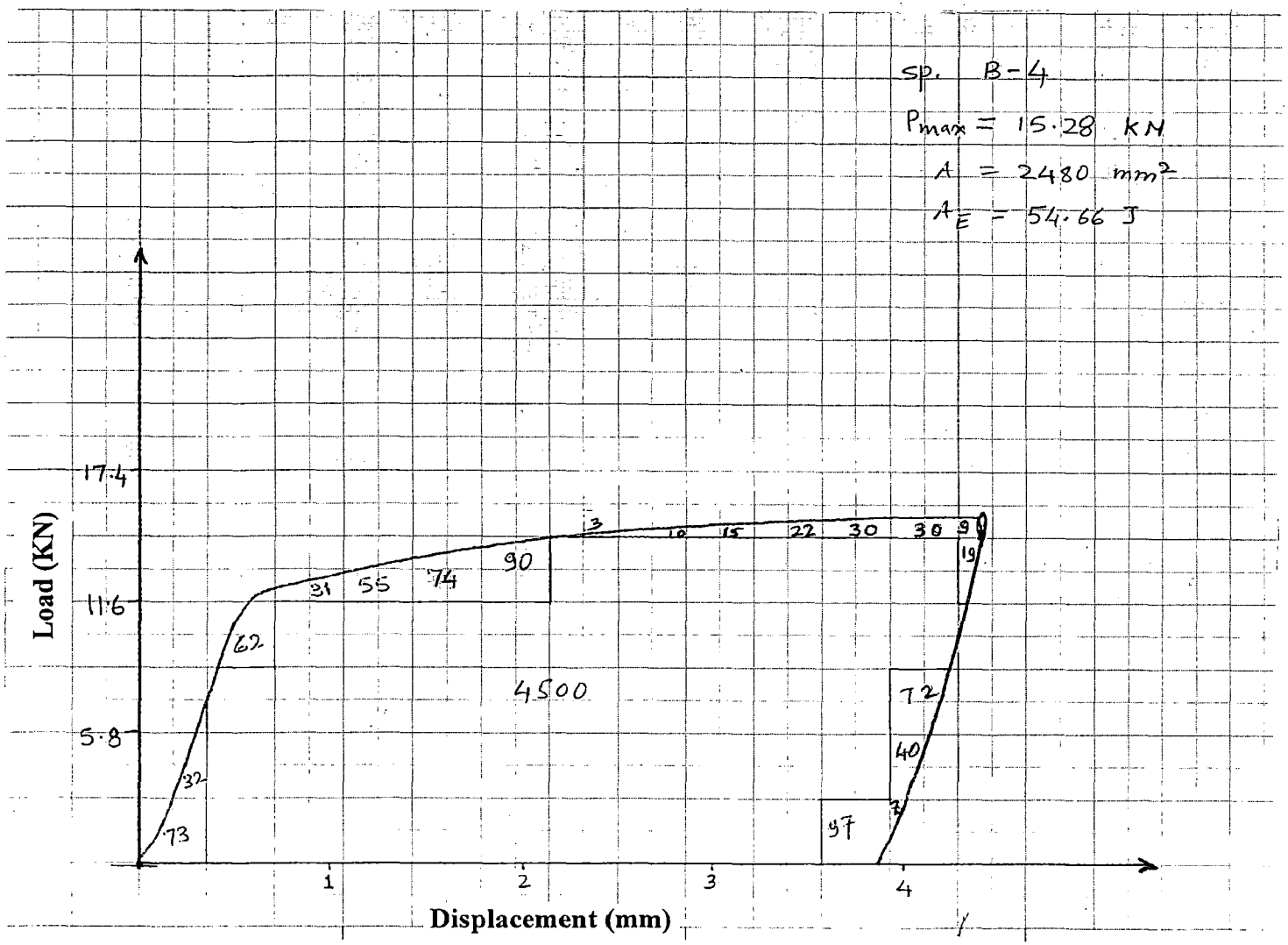

Fig. 4.14 Load displacement curve for base metal specimen B-4 of J_{1C} test.

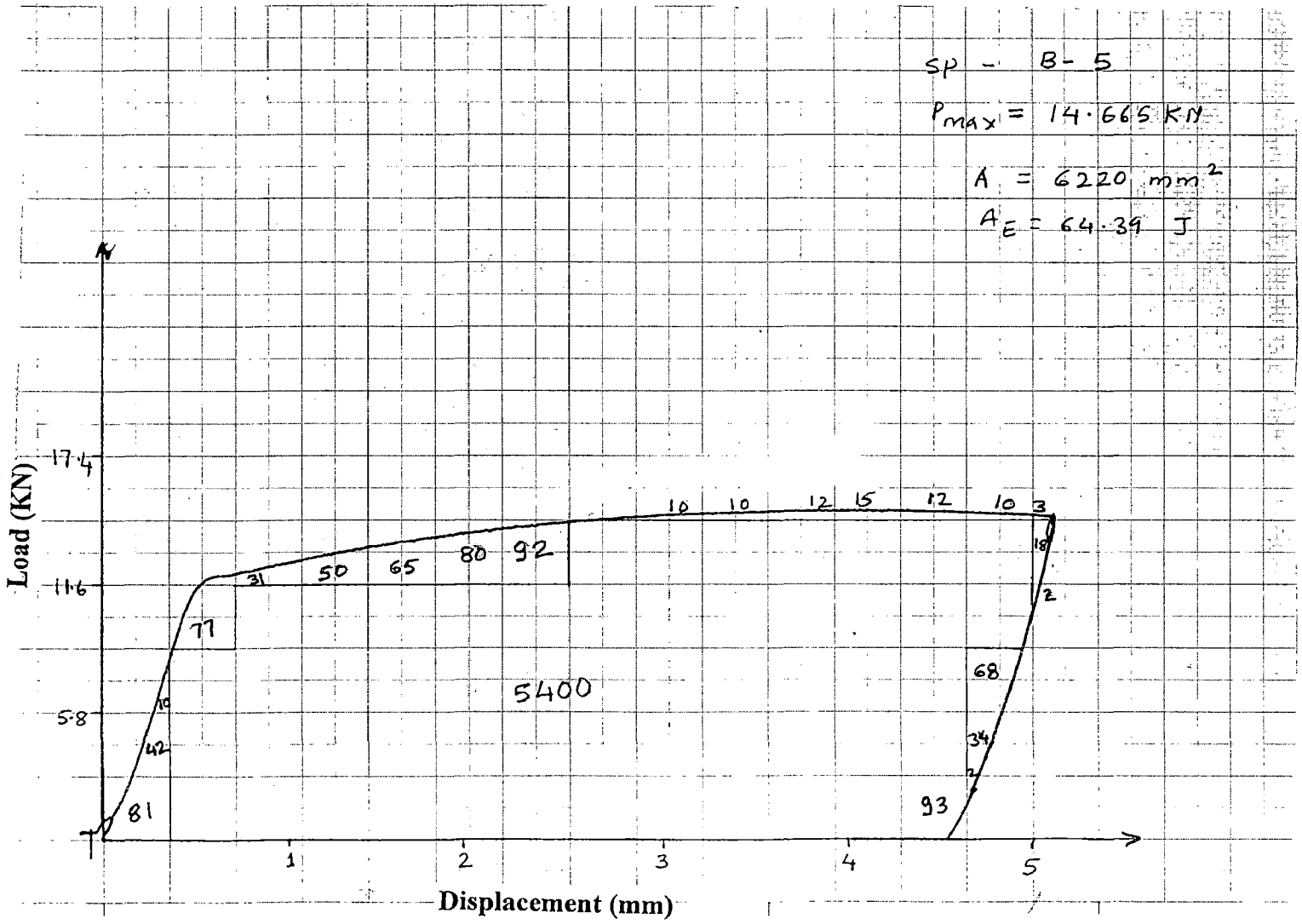

Fig. 4.15 Load displacement curve for base metal specimen B-5 of J_{IC} test.

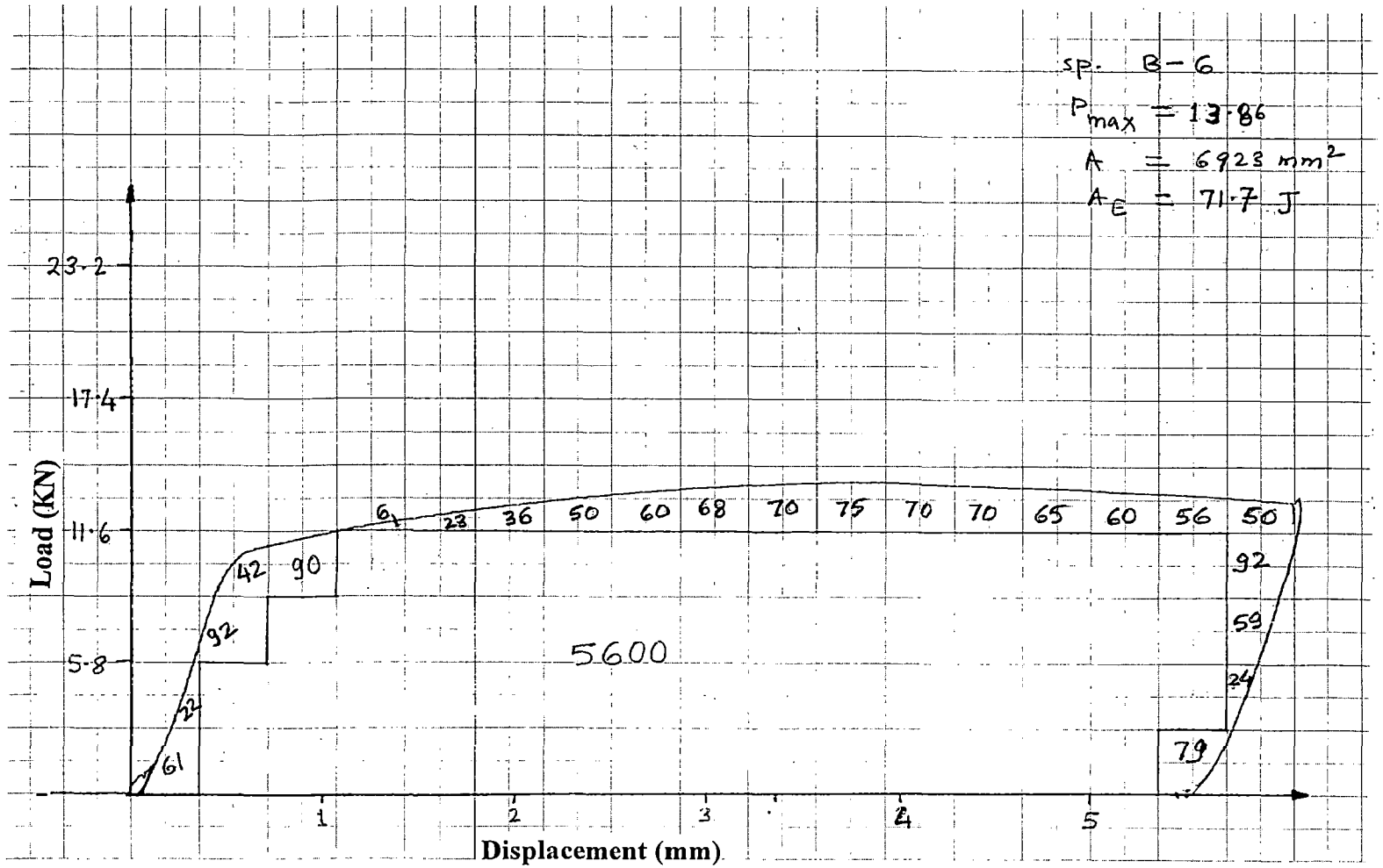

Fig. 4.16 Load displacement curve for base metal specimen B-6 of J_{IC} test.

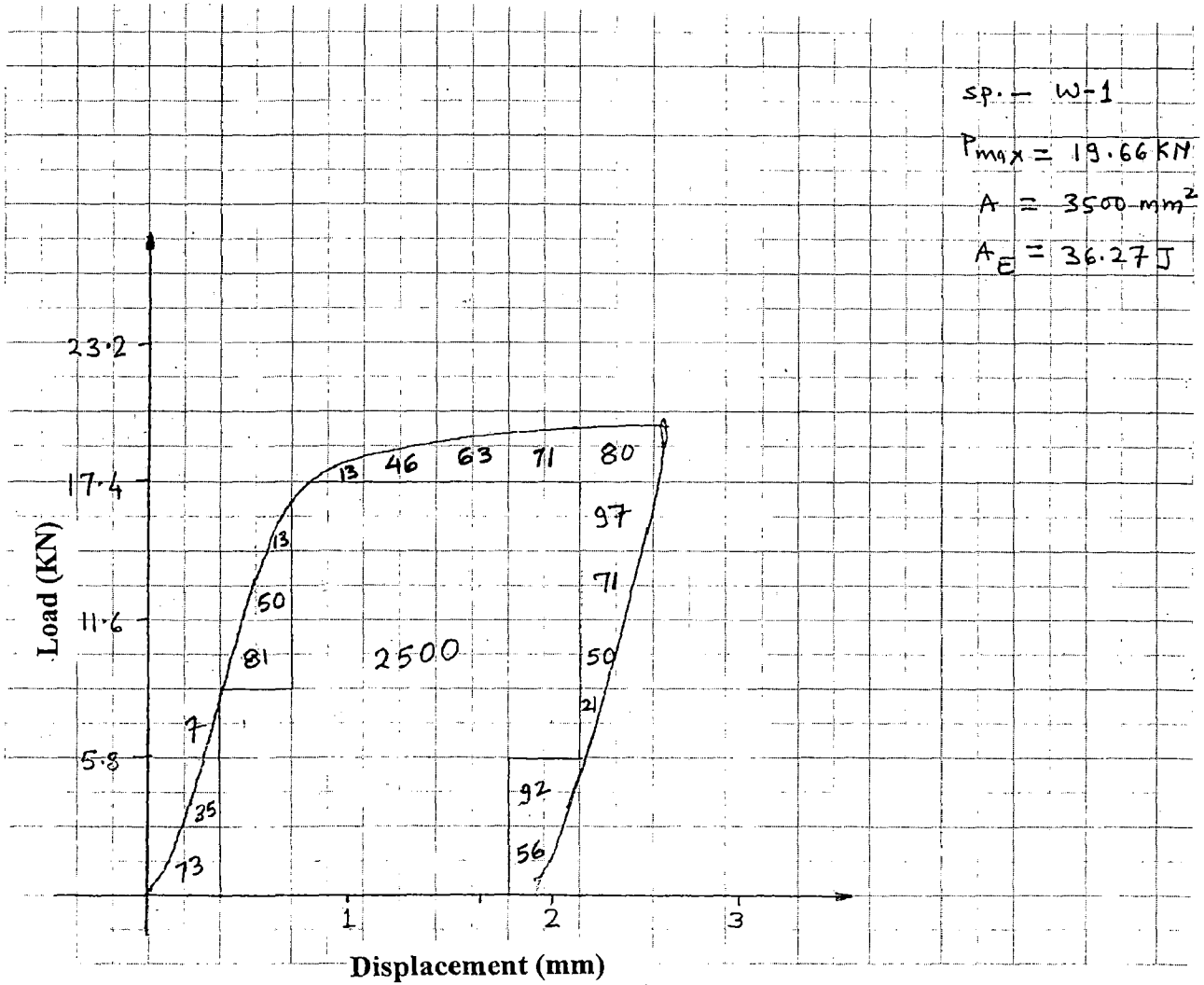

Fig. 4.17 Load displacement curve for weld metal specimen W-1 of J_{IC} test.

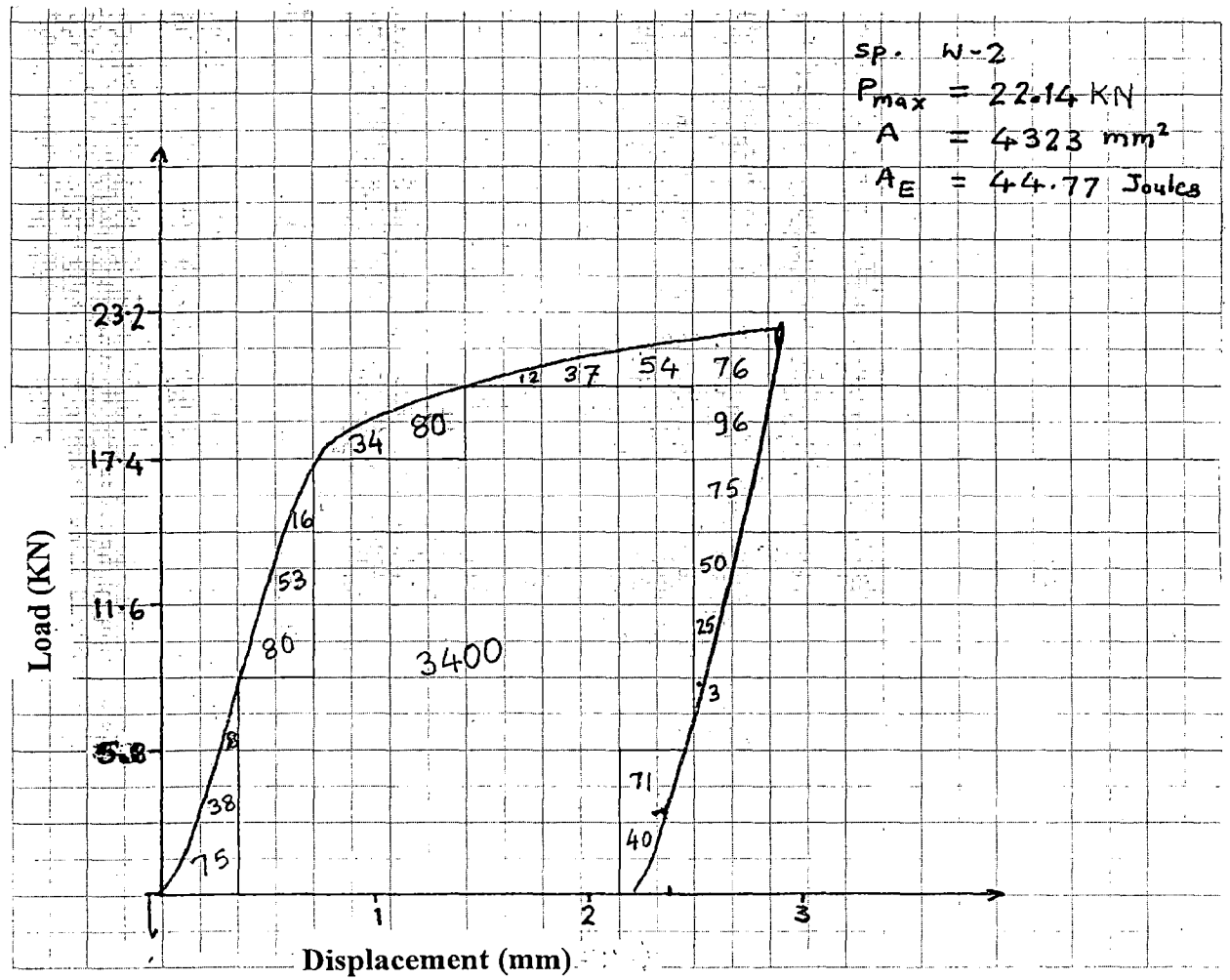

Fig. 4.18 Load displacement curve for weld metal specimen W-2 of J_{IC} test.

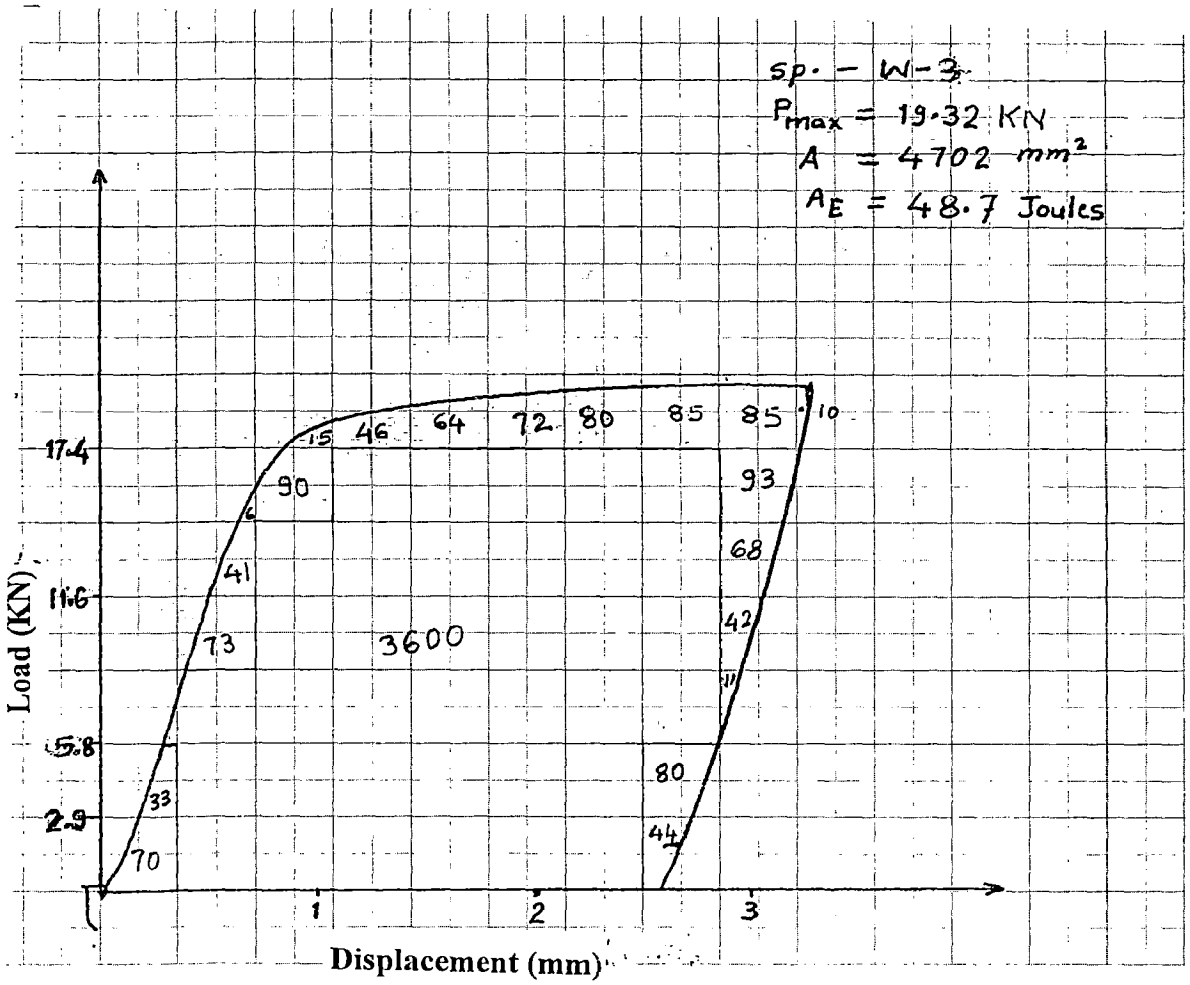

Fig. 4.19 Load displacement curve for weld metal specimen W-3 of J_{IC} test.

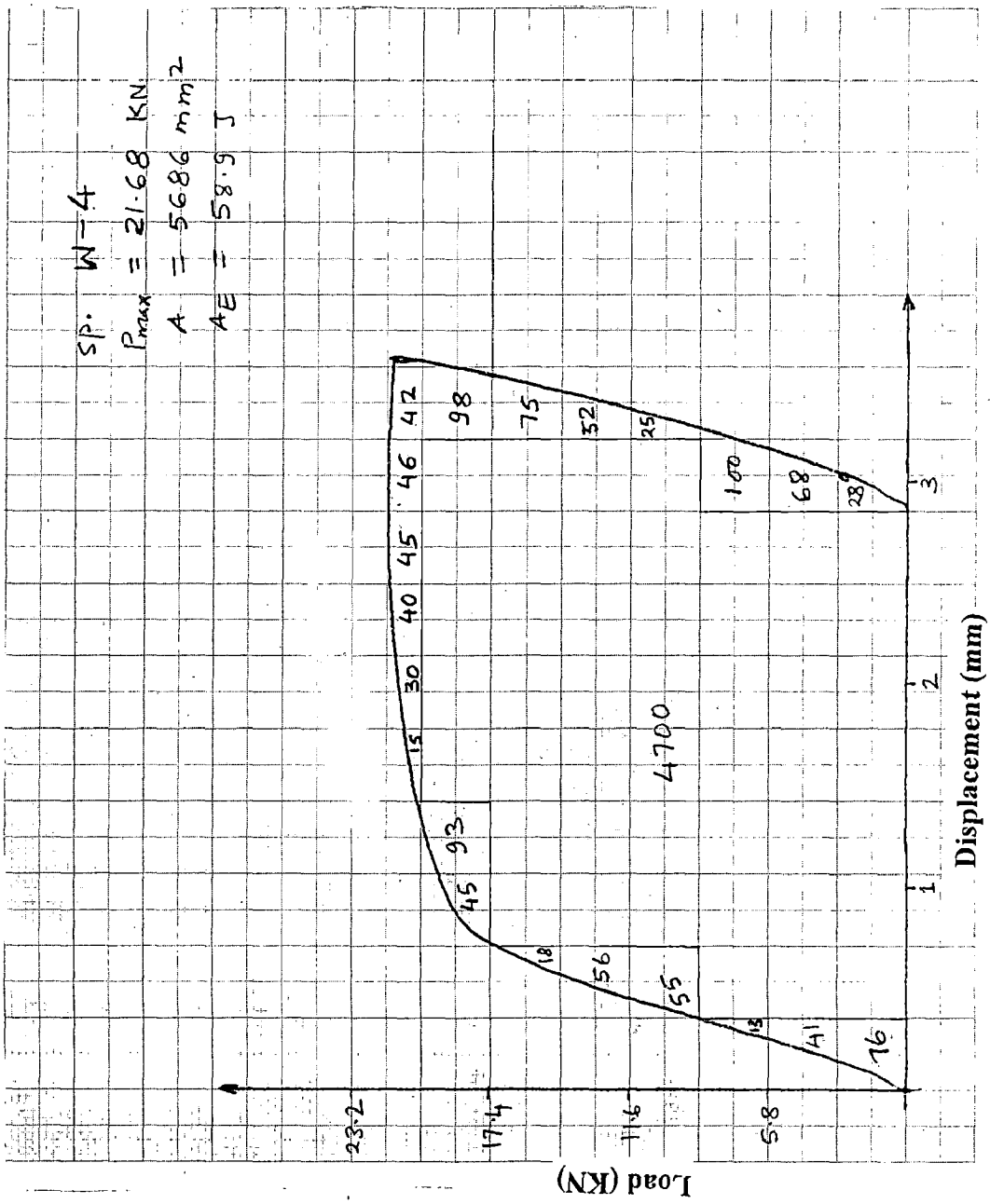

Fig. 4.20 Load displacement curve for weld metal specimen W-4 of J_{IC} test.

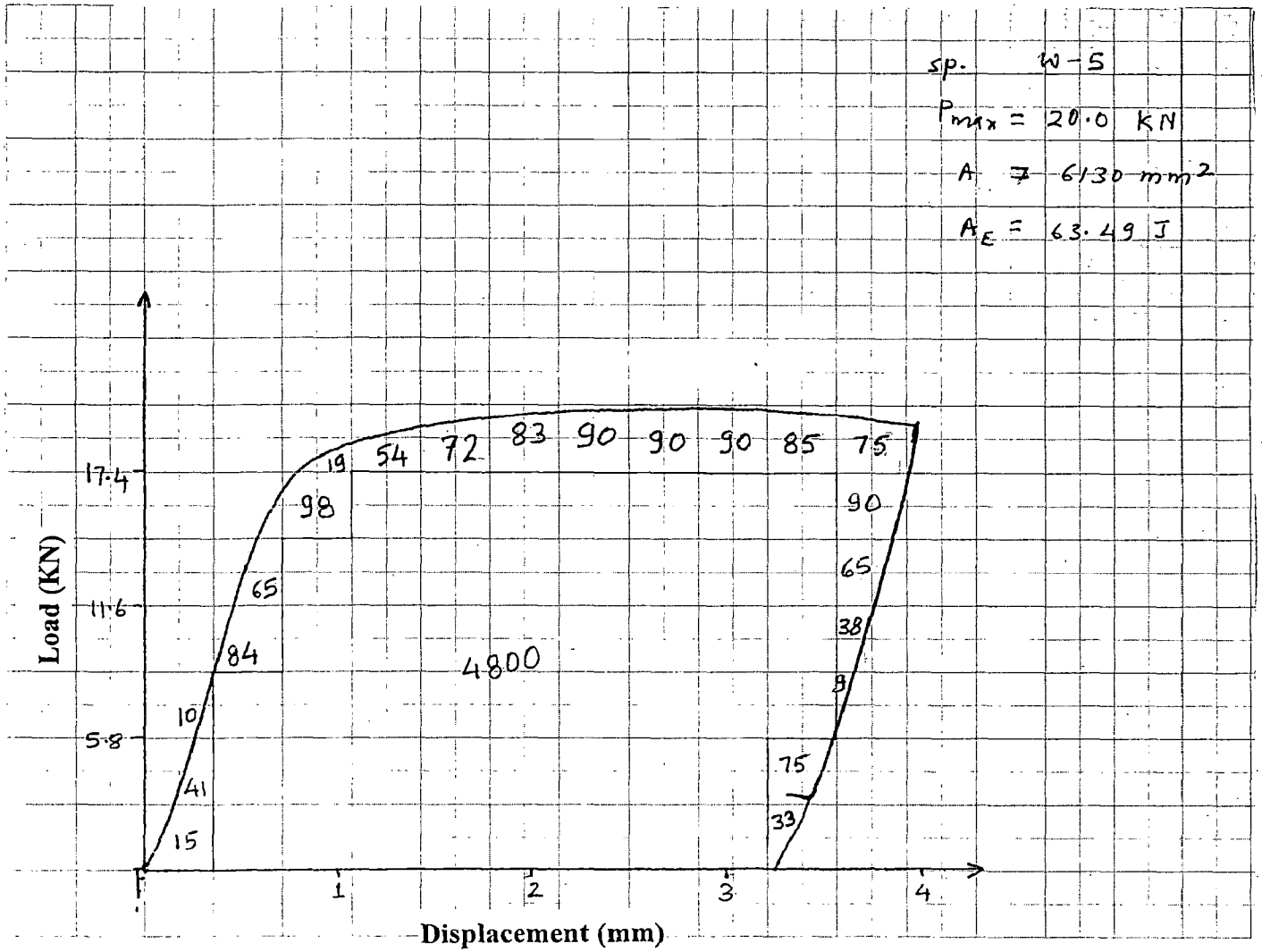

Fig. 4.21 Load displacement curve for weld metal specimen W-5 of J_{IC} test.

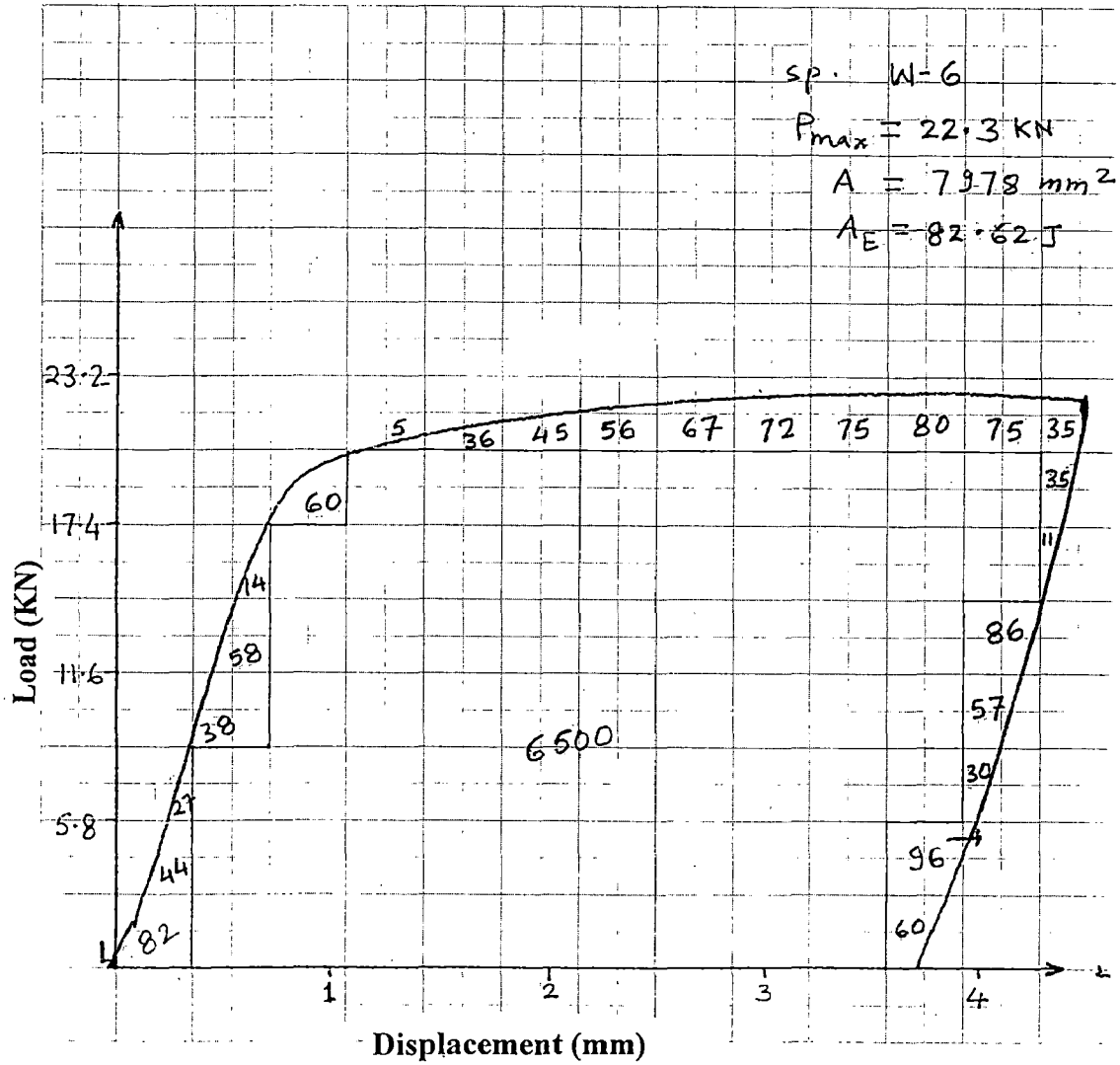

Fig. 4.22 Load displacement curve for weld metal specimen W-6 of J_{IC} test.

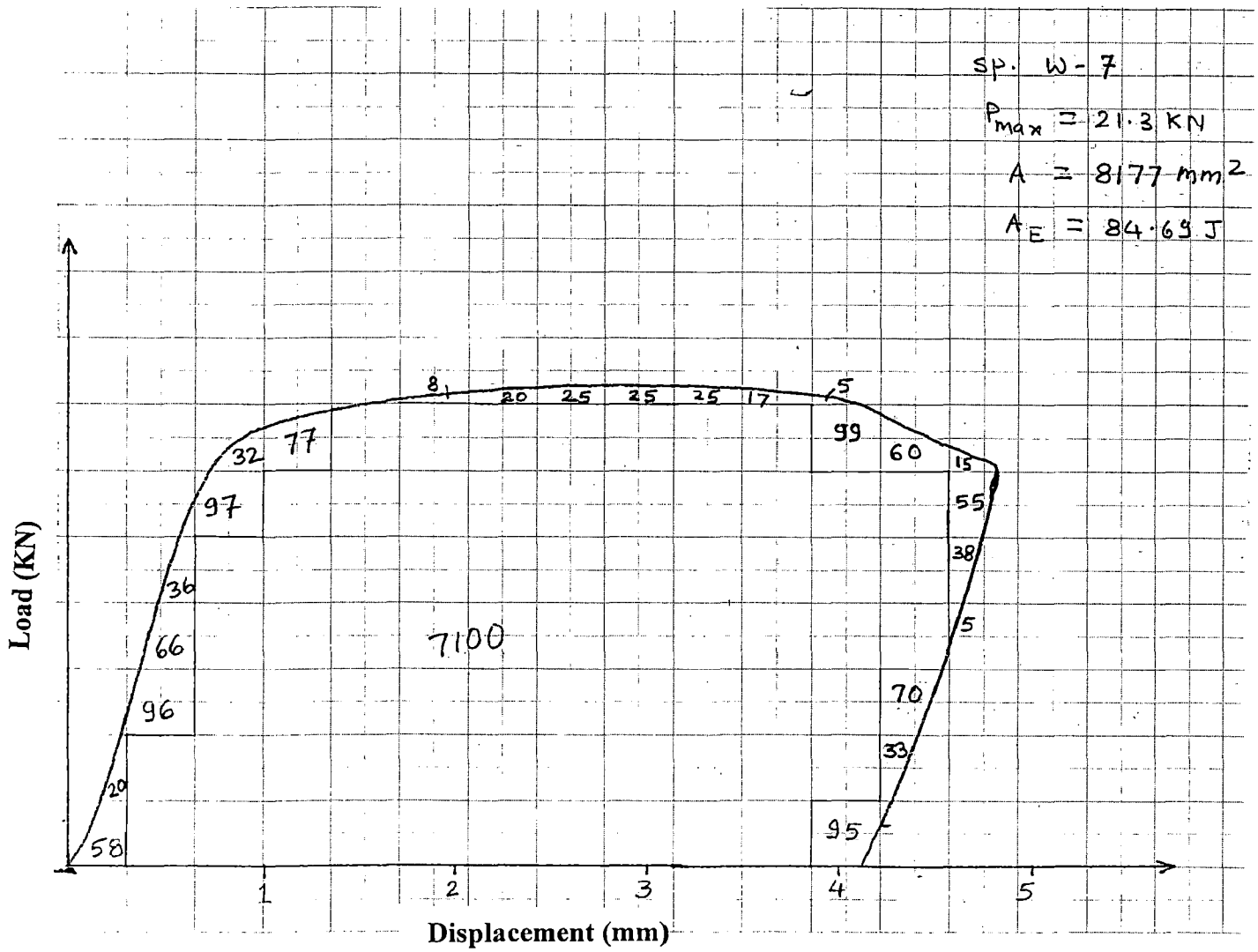

Fig. 4.23 Load displacement curve for weld metal specimen W-7 of J_{IC} test.

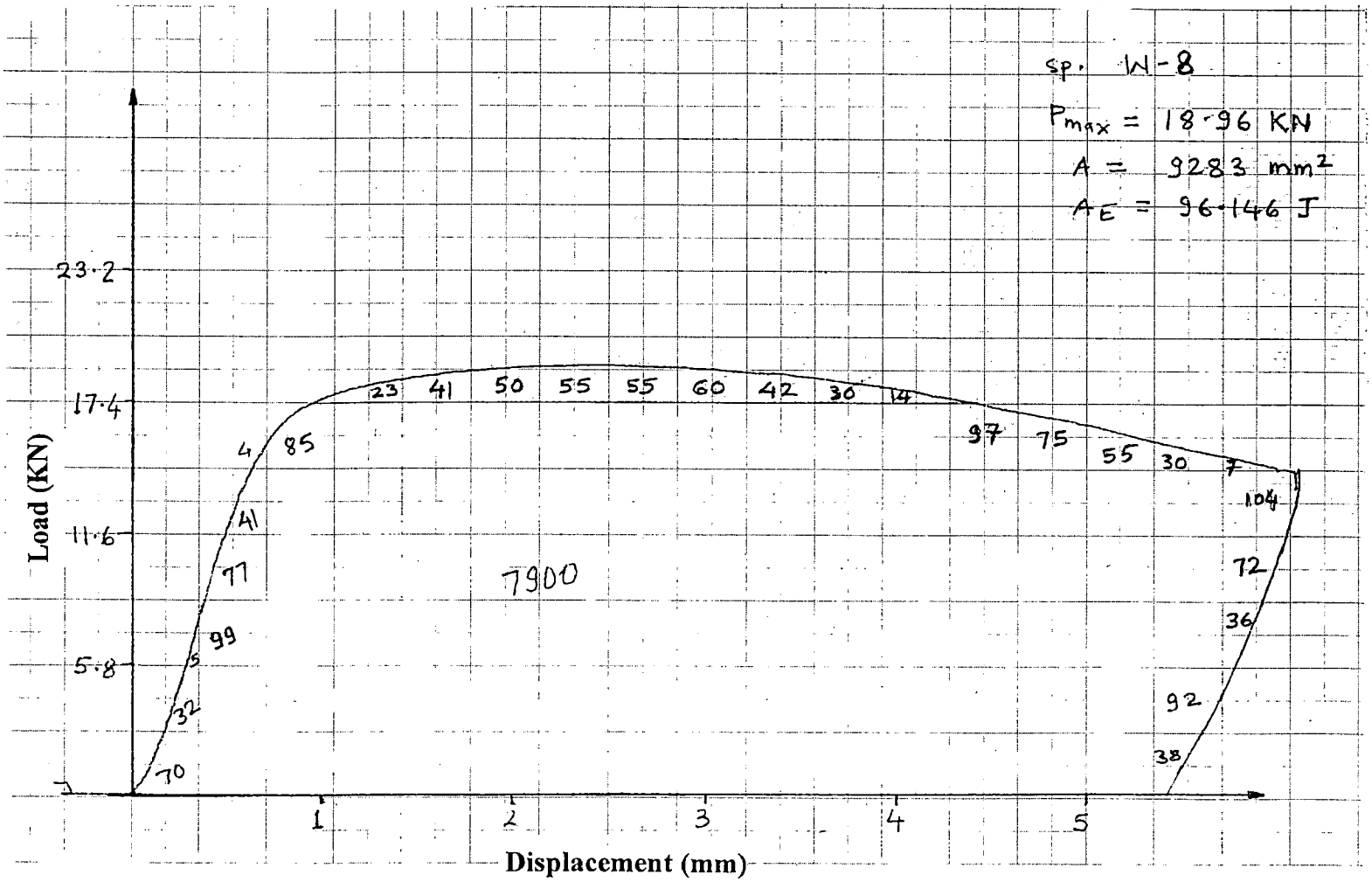

Fig. 4.24 Load displacement curve for weld metal specimen W-8 of J_{IC} test.

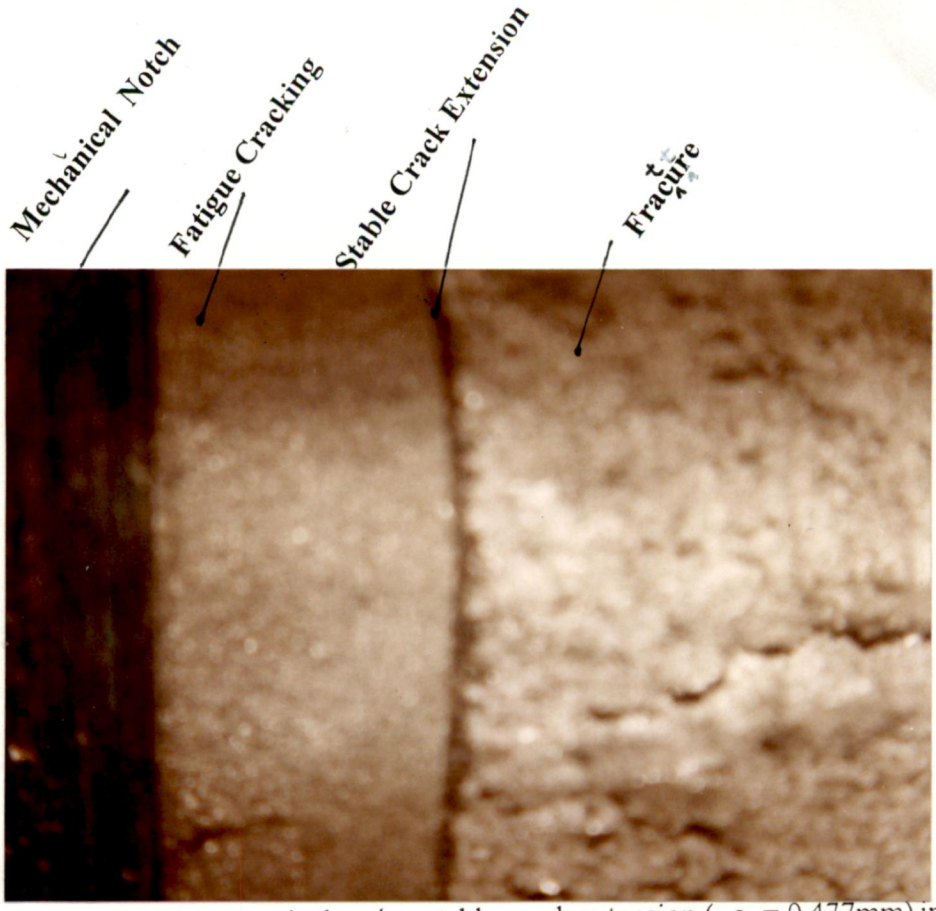

Fig. 4.25 Typical photograph showing stable crack extension (Δa_p = 0.477mm) in C-Mn Steel.

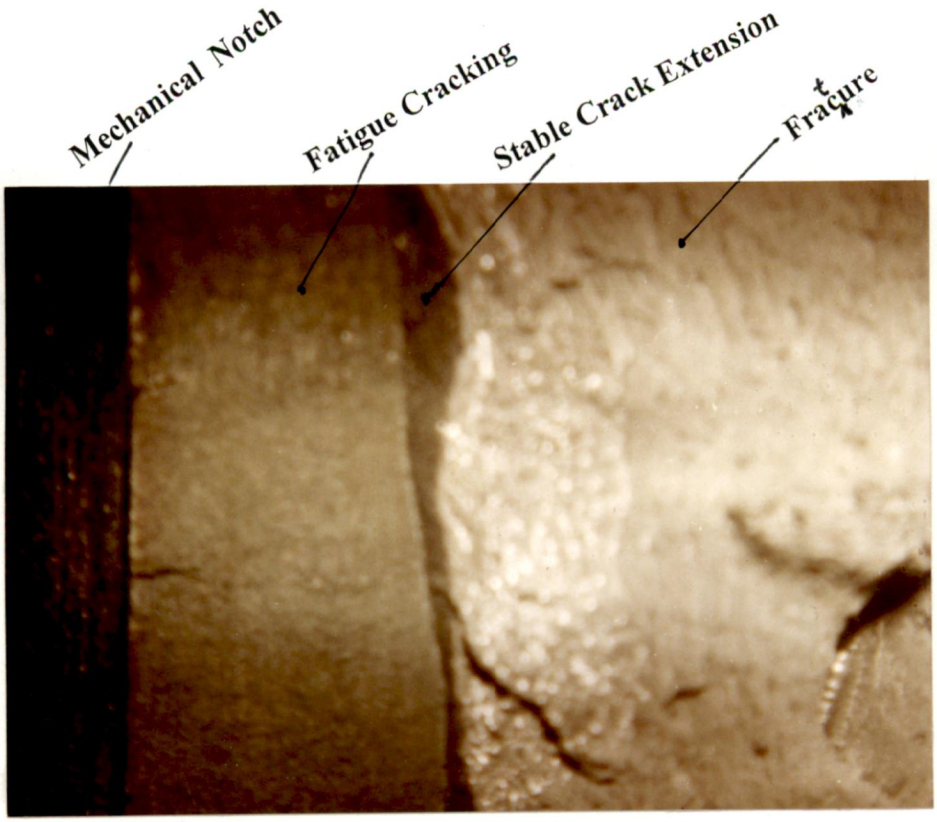

Fig. 4.26 Typical photograph showing stable crack extension (Δa_p = 0.56 mm) in C-Mn Stee

weld.

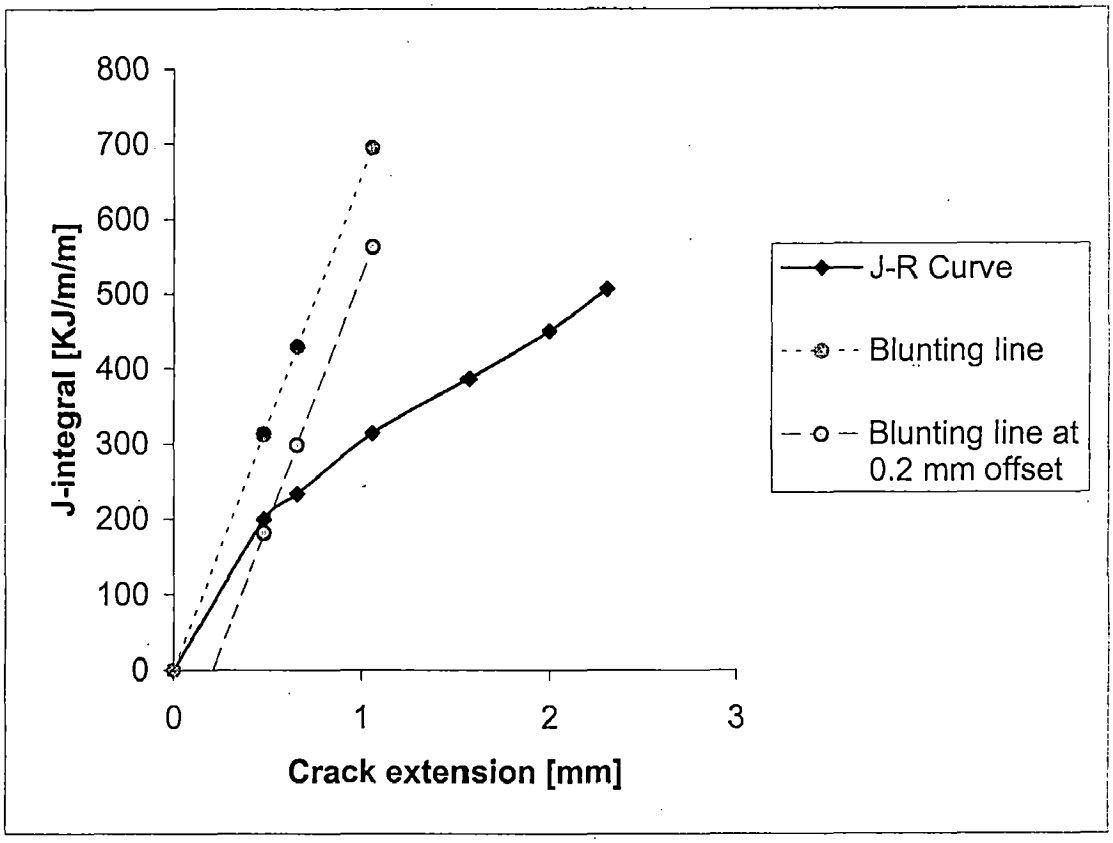

Fig.4.27 J_R- curve for base metal with blunting line $J = 2\sigma_y \Delta a$.

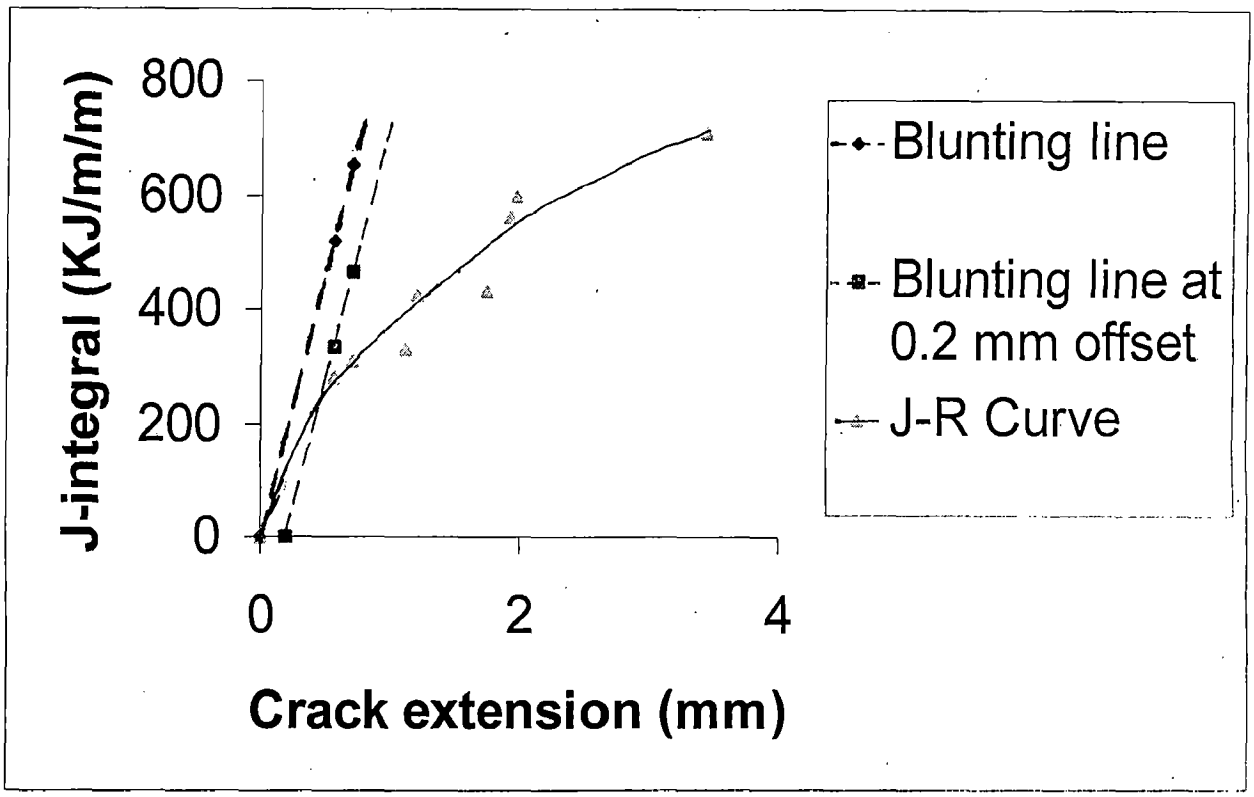

Fig.4.28 J_R- curve for weld metal with blunting line $J = 2\sigma_y \Delta a$.

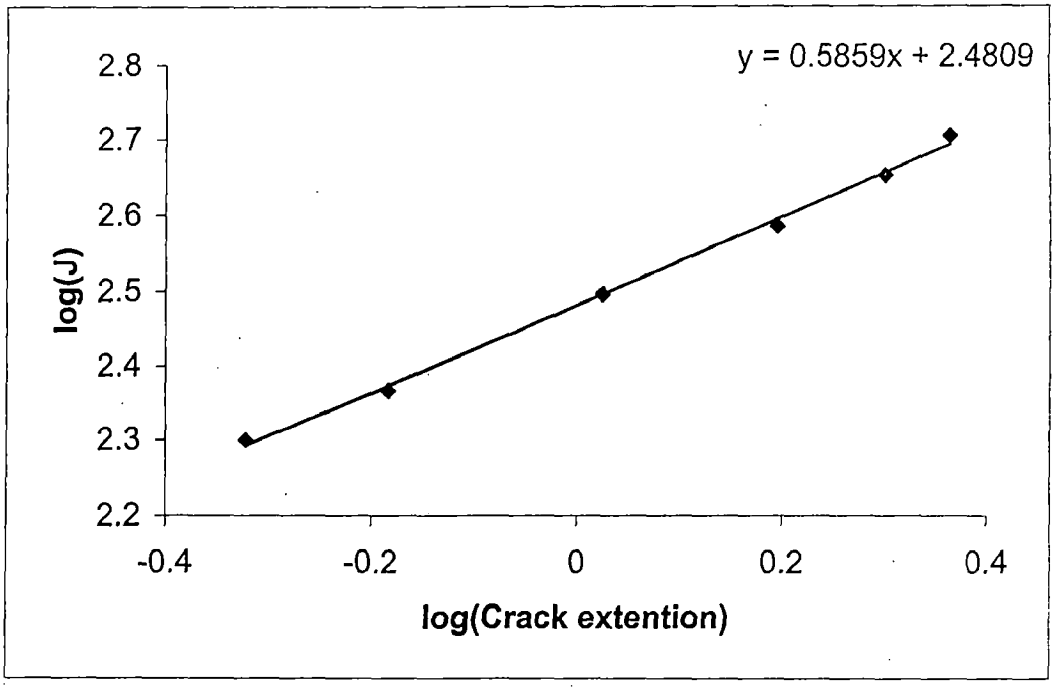

Fig. 4.29 J_R- curve for base metal on log-log scale.

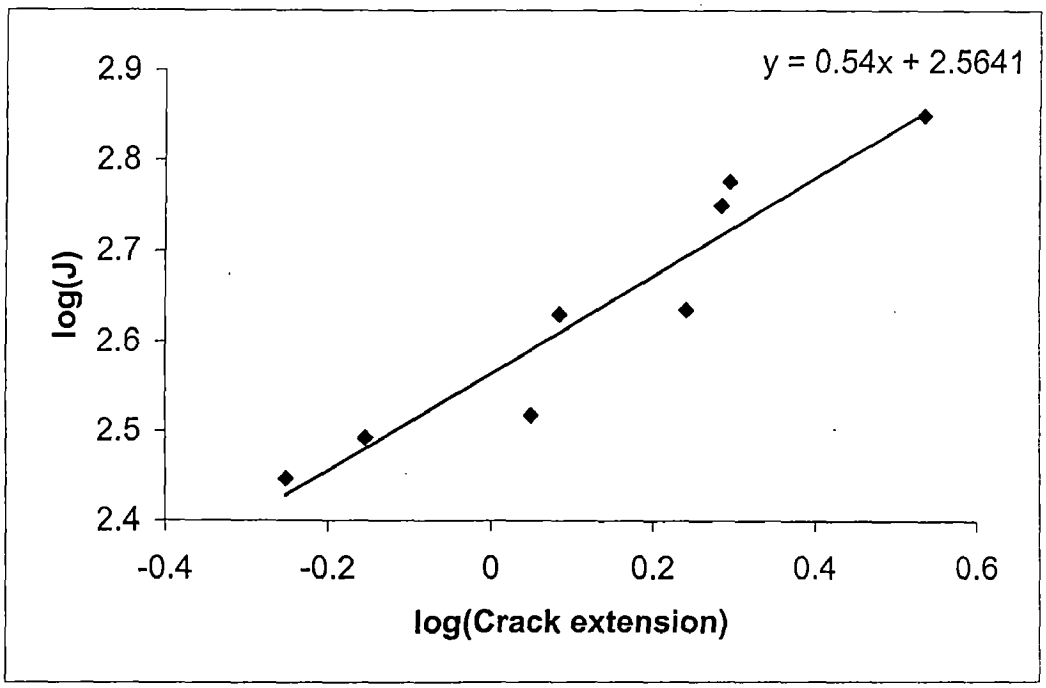

Fig. 4.30 J_R- curve for weld metal on log-log scale.